

2014

INVESTIGATION INTO THE CELLULAR ACTIONS OF CARNOSINE AND C-PEPTIDE

Emma H. Gardner
gardner36@marshall.edu

Follow this and additional works at: <http://mds.marshall.edu/etd>

 Part of the [Analytical Chemistry Commons](#), and the [Biochemistry Commons](#)

Recommended Citation

Gardner, Emma H., "INVESTIGATION INTO THE CELLULAR ACTIONS OF CARNOSINE AND C-PEPTIDE" (2014). *Theses, Dissertations and Capstones*. Paper 868.

This Thesis is brought to you for free and open access by Marshall Digital Scholar. It has been accepted for inclusion in Theses, Dissertations and Capstones by an authorized administrator of Marshall Digital Scholar. For more information, please contact zhangj@marshall.edu.

**INVESTIGATION INTO THE CELLULAR ACTIONS OF
CARNOSINE AND C-PEPTIDE**

**A thesis submitted to
the Graduate College of
Marshall University**

**In partial fulfillment of
the requirements for the degree of
Master of Science**

in

Chemistry

by

Emma H. Gardner

Approval by

Dr. Leslie Frost, Committee Chairperson

Dr. Derrick Kolling

Dr. Menashi Cohenford

Marshall University

May 2014

Table of Contents

List of Tables	iv
List of Figures	v
IRB Letter	vii
Abstracts	viii
1. Investigation into the Cellular Actions of Carnosine	1
Introduction	1
Experimental Methods	11
Preparation of Carnosine Affinity Beads	11
Tissue Lysis	12
Protein Isolation	13
SDS PAGE Analysis of Isolated Proteins	13
Preparation of Tryptic Digests of Protein Samples from SDS-PAGE Bands	13
Analysis of Tryptic Digests of Proteins by MALDI-TOF Mass Spectrometry	14
Analysis of Tryptic Peptide Amino Acid Sequences by LC/ESI/MS	15
Determining the Effect of Carnosine on AGE Structure Formation	15
Sodium Borohydride Reduction	16
UV-VIS Absorbance Profile of Hemin	16
Results and Discussion	16
Identification of Carnosine Binding Proteins Isolated from Bovine Kidney Tissue	16
Identification of Carnosine Binding Proteins Isolated from Mouse Kidney Tissue	24
Effect of Carnosine on the Formation of AGEs	28
Analysis of Carnosine-Hemin Interactions	33
Future Work	34
References	36
2. Proinsulin C-Peptide as an Active Biomolecule	38
Introduction	38
Experimental Methods	46
Preparation of C-Peptide Affinity Beads	46
Tissue Lysis	47
Protein Isolation	47
SDS PAGE Analysis of Isolated Proteins	48

Preparaion of Tryptic Digests of Protein Samples from SDS-PAGE Bands	48
Analysis of Tryptic Digests of Proteins by MALDI-TOF Mass Spectrometry	49
Analysis of Tryptic Digests of Proteins by LC/ESI/MS	49
Results and Discussion	50
Results from Trial 1 Using Tris Pre-clear Beads	52
Proteins Isolated from Kidney Tissue by C-peptide Beads	53
Proteins Isolated from Liver Tissue by C-peptide Beads	58
Results from Trial 2 using Bradykinin Pre-clear Beads	61
Proteins Isolated from Liver Tissue by C-peptide Beads	63
Proteins Isolated from Kidney Tissue by C-peptide Beads	65
References	71
Appendix A	73
Results from Earlier Trials for Heart Tissue Lysates	73

List of Tables

1.1 Glycated peptides in Cytochrome C identified by MALDI-TOF and LC/ESI/MS/MS	9
1.2. Carnosine-binding proteins identified by mass spectrometry	20

List of Figures

1.1. Structure of the dipeptide carnosine	1
1.2. Structure of the heme b	2
1.3. Overview of various oxidative stress-related effects	4
1.4. Glycation	6
1.5. MALDI-TOF mass spectra of the +2 ion of bovine Cyt	10
1.6. Basic experimental protocol for protein isolation	18
1.7. SDS-PAGE gel separation of proteins	18
1.8. MALDI-TOF peptide fingerprint mass spectrum for band 1	20
1.9. Binding of haptoglobin to hemoglobin	21
1.10. MALDI-TOF peptide fingerprint mass spectrum for band 2	22
1.11. TCP-1 chaperonin with its eight different subunits	23
1.12. MALDI-TOF peptide fingerprint mass spectrum for band 3	24
1.13. The Peptide Mass Fingerprint spectra for 20 kDa	26
1.14. The structure of HBB	27
1.15. The structure of the hemoglobin	27
1.16. MALDI-TOF mass spectra of the +2 ion of glycated cytochrome c	29
1.17. MALDI-TOF tryptic peptide mass fingerprint spectra of cytochrome C	30
1.18. MALDI-TOF tryptic peptide mass fingerprint spectra of cytochrome C	31
1.19. Space-filling plot of the horse cytochrome C structure	32
1.20. UV-VIS absorption profile of hemin in saturated carnosine solution	34
2.1. Structure of insulin C-peptide	38
2.2. Proinsulin structure	39
2.3. Insulin biosynthesis pathway	40
2.4. Proposed mechanism for C-peptide signaling cascade	42
2.5. Depiction of the role of C-peptide in atherosclerosis	43
2.6. Basic experimental protocol	51
2.7. SDS-PAGE Gel separation of proteins	53
2.8. MALDI-TOF peptide fingerprint mass spectrum for kidney 25 kDa	55
2.9. The amino acid sequence for E2	56
2.10. Schematic of oxidation decarboxylation of pyruvate	56
2.11. MALDI-TOF peptide fingerprint mass spectrum for kidney 50 kDa	57
2.12. Basic reaction catalyzed by long-chain specific acyl-CoA dehydrogenase	58

2.13. MALDI-TOF peptide fingerprint mass spectrum at liver 50 kDa	59
2.14. MALDI-TOF peptide fingerprint mass spectrum for liver 100 kDa	61
2.15. The amino acid structure of the peptide Bradykinin	62
2.16. SDS-PAGE Gel separation of proteins	63
2.17. MALDI-TOF peptide fingerprint mass spectra for liver 50 kD	64
2.18. MALDI-TOF peptide fingerprint mass spectrum for kidney 40 kD	65
2.19. MALDI-TOF peptide fingerprint mass spectrum for kidney 25 kD	67
2.20. The Matrix Mascot search results for the matched peptide sequences	67
2.21. CID mass spectrum recorded on the $(M+2H)^{+2}$ ion at m/z 919	68
2.22. Structure of lipoic acid	70
A.1. SDS-PAGE gel of proteins isolated from mouse heart	74
A.2. MALDI-TOF peptide fingerprint mass spectrum for 55 kDa	75
A.3. MALDI-TOF peptide fingerprint mass spectrum for 30 kDa	76
A.4. The reaction catalyzed by GAPDH as part of the glycolysis cycle	77

Office of Research Integrity

May 9, 2014

Emma H. Gardner
1133 Emerald Rd
Charleston, WV 25314

Dear Ms. Gardner:

This letter is in response to the submitted thesis abstract entitled “*Investigations into the Cellular Actions of Carnosine and Proinsulin C-Peptide.*” After assessing the abstract it has been deemed not to be human subject research and therefore exempt from the oversight of the Marshall University Institutional Review Board (IRB). The Code of Federal Regulations (45CFR46) has set forth the criteria utilized in making this determination. If there are any changes to the abstract you provided then you would need to resubmit that information to the Office of Research Integrity for a review and determination.

I appreciate your willingness to submit the abstract for determination. Please feel free to contact the Office of Research Integrity if you have any questions regarding the future protocols that may require IRB review.

Sincerely,

A handwritten signature in blue ink that reads "Bruce Day". The signature is written in a cursive style with a large, stylized "D" at the end.

Bruce F. Day, ThD, CIP
Director

Abstracts

1. Investigation into the Cellular Actions of Carnosine

Carnosine is a dipeptide composed of beta-alanine and histidine found exclusively in long-lived animal tissues. The cellular action of carnosine is still under extensive investigation; however, it has been proposed to have a role as an anti-oxidant and oxygen free radical scavenger, a physiological buffer, a heavy metal chelator, and has been implicated as an anti-aging agent.^{2,4} Our lab has been studying the interaction between carnosine and heme by analyzing both the effect carnosine has on the glycation of the heme containing protein cytochrome c and the interaction of carnosine with free hemin. We have observed that the addition of carnosine to glycated cytochrome c inhibits the formation of advanced glycation end product (AGE) structures. We have also found that the addition of carnosine to a solution of free hemin drastically increases the solubility of hemin and causes a shift of the λ_{\max} in its UV-Vis absorbance profile. We propose that carnosine is a natural intracellular heme chelator and that this interaction may act as a signal for cellular antioxidant processes. We have designed an experiment to identify proteins capable of binding to carnosine and heme-chelated carnosine. Using mass spectral techniques, we were able to identify a protein isolated from kidney tissue lysates using carnosine affinity beads. By identifying a carnosine protein binding partner, we gained a better understanding of the cellular action of carnosine that may eventually lead to the development of novel drugs for the treatment of a variety of diseases in which oxidative injury and cellular stress occurs.

2. Proinsulin C-Peptide as an Active Biomolecule

Proinsulin C-peptide was thought to be an inert species whose only purpose was for proper binding of insulin; however, now C-peptide is believed to be an important, biologically active molecule that can improve some of the complications associated with diabetes mellitus. In addition, type-1 patients who are able to maintain C-peptide levels have fewer complications and better glycemic control. The goal of this project was to gain a better understanding of the biochemical mechanism of action of C-peptide by identifying cellular proteins in varying types of tissue cell lysates capable of binding to the proinsulin C-peptide. This experiment was performed via creating C-peptide affinity beads by attaching C-peptide to NHS magnetic beads via the peptide's N-terminus. Once attached, cellular lysates of varying tissue types were incubated with the affinity beads. Any bound proteins are eluted, separated by reducing SDS-PAGE, digested with trypsin, and identified via Protein Mass Fingerprint spectra obtained from the MALDI-TOF mass spectrometer. We were able to successfully identify several proteins from mouse kidney, liver, and heart tissue lysates that were isolated with the C-peptide affinity beads. The identification of these proteins has given us a better understanding of the purpose of C-peptide in the body and how it is related to diabetes and other glucose related diseases. We found that the C-peptide seems to play a role in increasing the antioxidant properties and glucose clearance rate within cells.

1. Investigation into the Cellular Action of Carnosine

Introduction:

Carnosine is a dipeptide composed of beta-alanine and histidine (Figure 1.1). Carnosine is found exclusively in animal tissue and is present in long-lived tissues, such as the brain and muscle, in surprisingly high concentrations (up to 20 mM).¹ Carnosine has been implicated as an anti-aging agent because it can delay senescence in cultured human fibroblasts and can reverse the senescent phenotype in cultured human cells.^{2,3} The cellular action of carnosine is still under extensive investigation; however, it has been proposed to have a role as an anti-oxidant and oxygen free radical scavenger, a physiological buffer, a heavy metal chelator, and an immunostimulant.⁴ Carnosine has also been proposed to act as a naturally occurring anti-glycating agent.⁵ Studies have shown that it can oppose the glycation of proteins and act to lessen some diabetic complications.

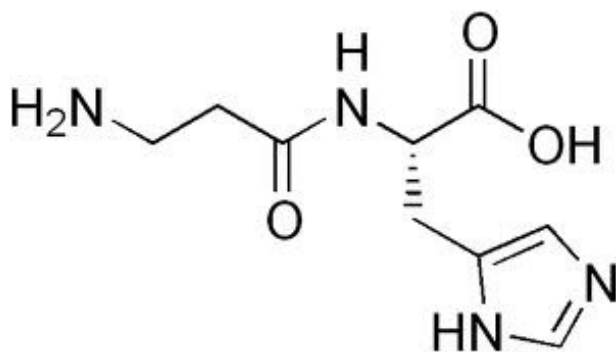


Figure 1.1. Structure of the dipeptide carnosine.

Heme molecules consist of an iron atom held in a porphyrin (Figure 1.2). They are a major component in hemoglobin in red blood cells as well as myoglobin in the muscles and cytochrome c.⁶ Heme b, the most common isoform, is present in hemoglobin, myoglobin and cytochrome b. Hemes are synthesized in the mitochondria and cytosol of immature red blood

cells.⁷ Free heme is toxic in that it catalyzes the oxidation, covalent cross-linking and aggregate formation of proteins, the formation of cytotoxic lipid peroxide via lipid peroxidation and damages DNA through oxidative stress.⁸ Heme toxicity can occur in a body with high levels of free heme in the blood plasma. This can be caused when a body absorbs exorbitant amounts of heme iron either from digesting animal meat or excessive intake of iron tablets. Genetic factors may predispose a body absorbing high amounts of heme. Hereditary hemochromatosis is the most common cause of heme toxicity. Some results of heme toxicity include heart problems, menstrual irregularity, chronic fatigue, joint pain, liver disease, diabetes, heart failure and cancer. Cells have methods to protect against heme toxicity such as through heme oxygenase-1 that catalyzes the degradation of heme in response to oxidative stress.⁹

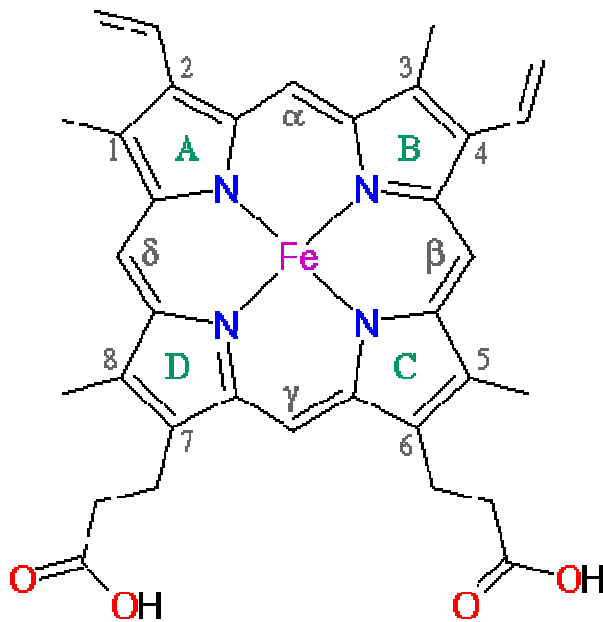


Figure 1.2. Structure of the heme b molecule present in proteins including hemoglobin, myoglobin, and cytochrome b.

Our lab has been studying the interaction between carnosine and heme by analyzing both the effect carnosine has on the glycation of the heme containing protein hemoglobin and the interaction of carnosine with free hemin. Hemin is an iron containing porphyrin that holds a heme b with a chloride ligand. It is used medically to combat porphyria, a rare medical disorder in which porphyrins cannot be properly produced to form hemes in the body. We have found that the addition of carnosine to a solution of free hemin drastically increases the solubility of hemin and causes a shift of the λ_{max} in its UV-Vis absorbance profile. We propose that carnosine is a natural intracellular heme binder, and that this interaction may act as a signal for cellular antioxidant processes. Perhaps carnosine or the heme-chelated carnosine may serve as a ligand for a nuclear receptor protein involved in the transcriptional regulation of a class of genes involved in a cellular protective/antioxidant pathway. For example, heme-chelated carnosine may upregulate the transcription of heme oxygenase 1 (HO-1), the essential enzyme in heme catabolism. Increased cellular HO-1 activity results in cytoprotection against oxidative injury and cellular stresses that would play a major role in cellular senescence.

An oxidative environment in a cell means that the cell is overproducing oxidative species. This can cause oxidative stress on a system. This can be harmful to a body and cause toxic effects through the production of free radicals and peroxides that can damage the cell.¹⁰ The most major of the long term effects is the damage of DNA. Metals such as iron are capable of catalyzing some redox cycle reactions via electron transfer process.

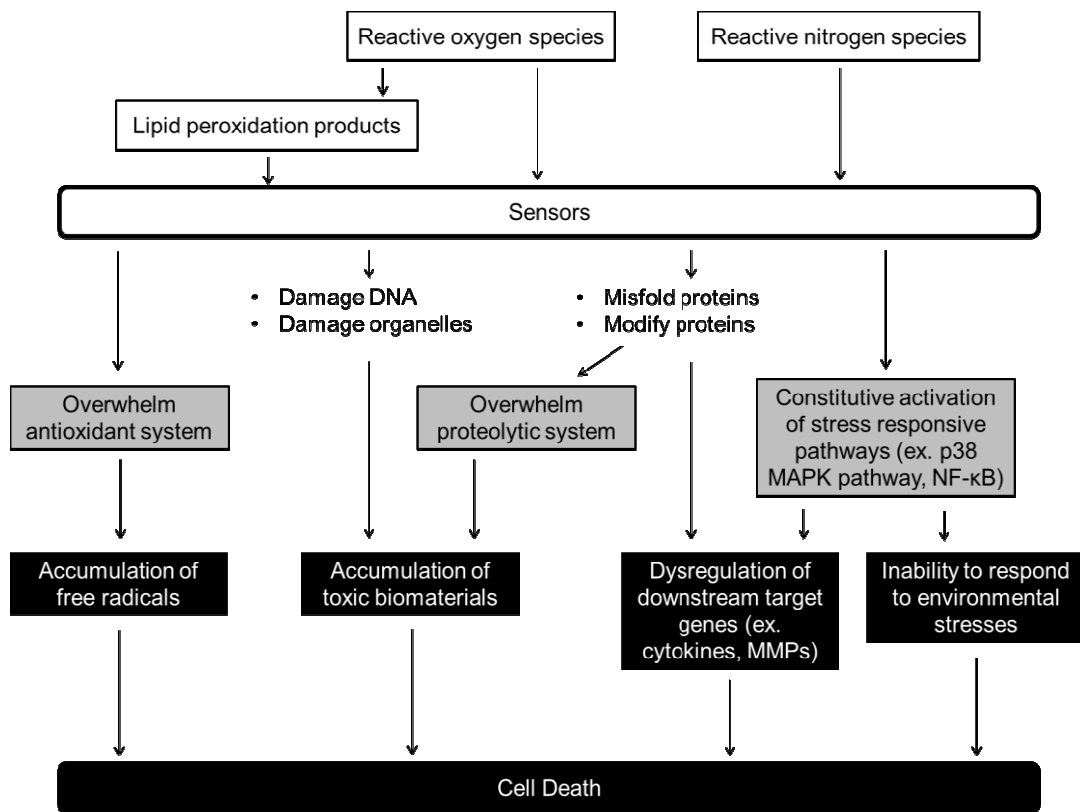


Figure 1.3. Overview of various oxidative stress-related effects on the cell, that would contribute to cell death.²⁵

An experiment was designed to identify cellular proteins capable of binding to carnosine and heme-chelated carnosine. A carnosine affinity column was developed by attaching carnosine to benzyloxybenzylbromide resins via the peptide's N-terminus. In addition, heme-chelated carnosine affinity beads were created by passing a solution of hemin through the carnosine affinity columns. Tissue samples were lysed and incubated with the affinity beads, and mass spectrometry was used to identify all the proteins capable of binding to these affinity beads. By identifying these protein-binding partners, a better understanding can be gained of the cellular action of carnosine and heme-chelated carnosine; this could eventually lead to the development of novel drugs for the treatment of a variety of diseases.

Spontaneous glycation of protein amines by sugars is a reaction that can lead to protein modification and dysfunction. The glycation of proteins begins with the formation of an

unstable Schiff base that occurs between the carbonyl group of the reducing sugars D-glucose or D-galactose and the free amino groups on proteins. This Schiff base then rearranges to form a more stable Amadori product that with time forms a heterogeneous group of compounds referred to as Advanced Glycation End Products (AGEs).¹¹⁻¹³ A schematic showing the formation of glycation products is shown in Figure 1.4. Protein glycation is influenced by many factors in vivo, including the nature and concentration of the carbonyl substrates, the availability and reactivity of the amino groups on proteins, and the chemical or enzymatic degradation of glycation products and their renal clearance.¹⁴⁻¹⁵

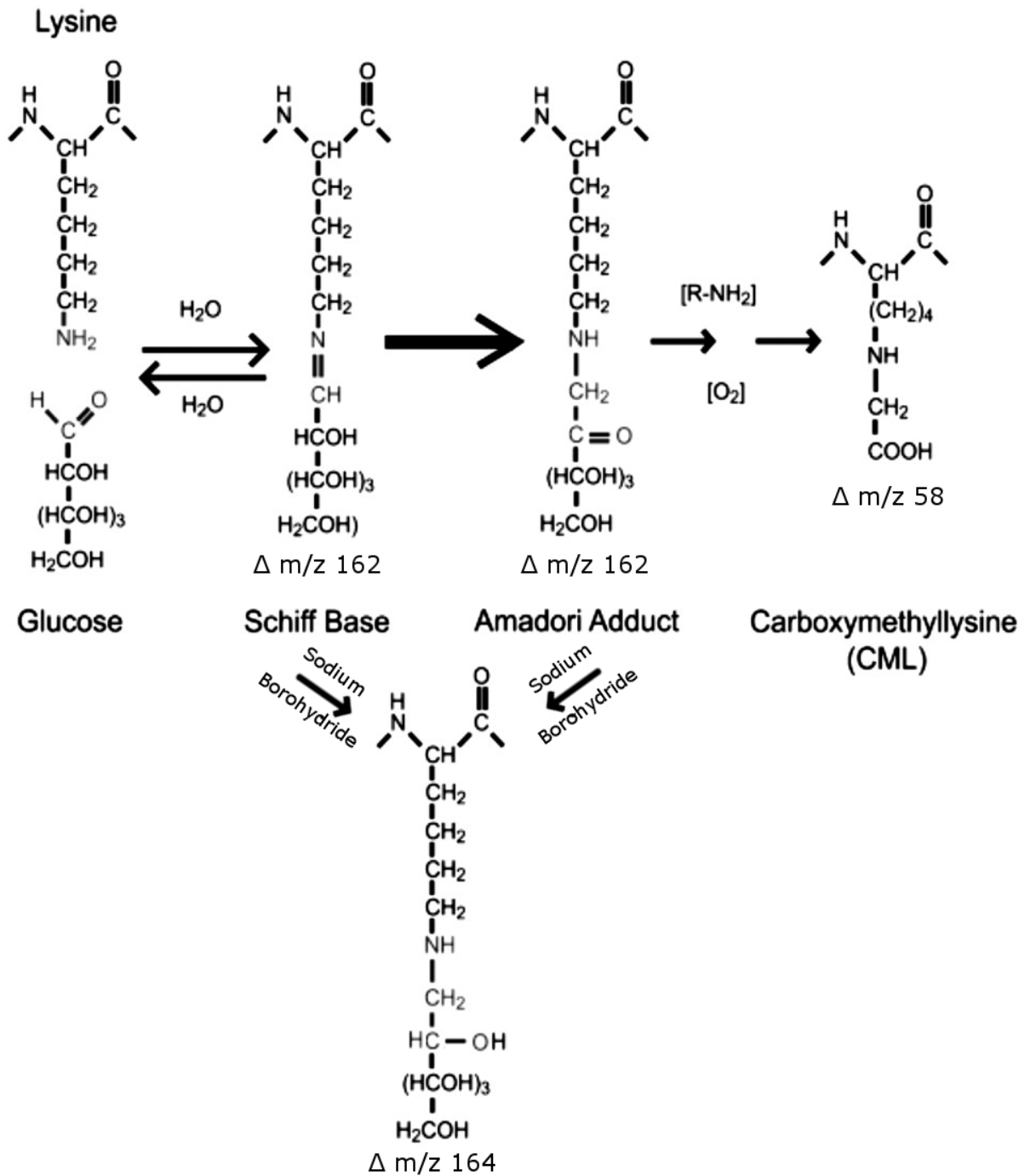


Figure 1.4. Glycation

Cytochrome c (cyt c), a c-type heme protein containing a heme moiety covalently attached to the polypeptide chain, plays a role in both cellular respiration and apoptosis. Cyt c, the only

nonintegral protein involved in the electron transport chain, associates with its respiratory partner cytochrome oxidase by use of a group of lysines rimming the heme edge allowing heme-to-heme contact needed for efficient electron transfer.¹⁶ ATP has been proposed to serve as an important inhibitory regulator of respiratory activity in the cell by shifting these lysines away from this interaction upon binding to cyt c.¹⁷ Cyt c is also a key player in the cellular apoptosis process in that one of the triggering events of apoptosis is the release of cyt c from the inner mitochondrial membrane into the cytosol of the cell. Additional lysines on the surface of cyt c have been shown to be important in the binding of cyt c to the membrane, and the glycation of these residues could interfere with its membrane binding properties and have an effect on the apoptosis process. Cyt c has a cluster of lysine residues surrounding the heme edge that are involved in the electrostatic interaction with negatively charged lipids. When bound to anionic lipids, cyt c orients the side bearing Lys-72, 86 and 87 towards the membrane surface with the heme favorably exposed for the electron transfer activity.¹⁸

We propose that the glycation of cyt c with D-galactose could alter critical functional lysine groups on this protein, leading to impaired functions in respiration and apoptosis. A student working in the Frost lab, Mr. Derrick Collins, has previously identified the preferential sites of glycation when cyt c was condensed with D-galactose *in vitro*. Table 1 below summarizes the data that he obtained and shows the sequences and the location of D-galactose in each of the glycated peptides observed. Mr. Collins also determined the effect of carnosine on the initial glycation of cytochrome c with D-galactose by monitoring the mass shifts that occurred when the protein was glycated (+162 Da/lactose addition). Protein samples incubated with D-galactose in the presence and absence of carnosine were analyzed daily for eleven days by MALDI-TOF mass spectrometry. The resultant mass spectra can be seen in Figure 1.5. The glycation pattern

when carnosine is added to the incubation mixture remains similar to when it is absent, indicating that carnosine does not inhibit the initial glycation reaction between cyt c and galactose. The glycation could only be monitored for 11 days, because the protein began to degrade in the constant presence of carnosine and galactose. Since carnosine did not inhibit the initial attachment of a sugar molecule to the cyt c protein, we propose that carnosine may be involved in protection against the formation of the advanced glycation endproducts that occurs over time after the sugar is added to the protein.

Table 1.1

Glycated peptides in Cytochrome C identified by MALDI-TOF and LC/ESI/MS/MS

Tryptic Digest Fragments	Peptide _{aa}	Theoretical Mass of Fragments in Da	MALDI-TOF Observed Mass in Da	$\Delta m/z$	Analysis by Tandem MS Incorporating CID
HK* TGPNLHGLFGR	26-38	1434	1598	164	²⁷ K
GGK* HK*<i>TGPNLHGLFGR</i>	23-38	1676	1840	164	²⁵ K & ²⁷ K (a)
EETLM♦ EYLENPK*K	61-73	1640	1804	164	⁷² K
K* TEREDLIAYLK	88-99	1479	1643	164	⁸⁸ K
KK* TEREDLIAYLK	87-99	1607	1771	164	⁸⁸ K
KK* TEREDLIAYLKK	87-100	1735	1899	164	⁸⁸ K

Galactated cytochrome C was prepared by incubating the native protein (1.0 mg) with D-galactose (35 mg) in 500 μ L of PBS, pH 7.4, for 24h at 37°C.

*Denotes that these sites represent galactated lysine residues.

♦Denotes that this site represents an oxidized methionine residue.

(a) The peptide at m/z 1840 was a mixture of two peptides, one with ²⁵K modified and one with ²⁷K modified.

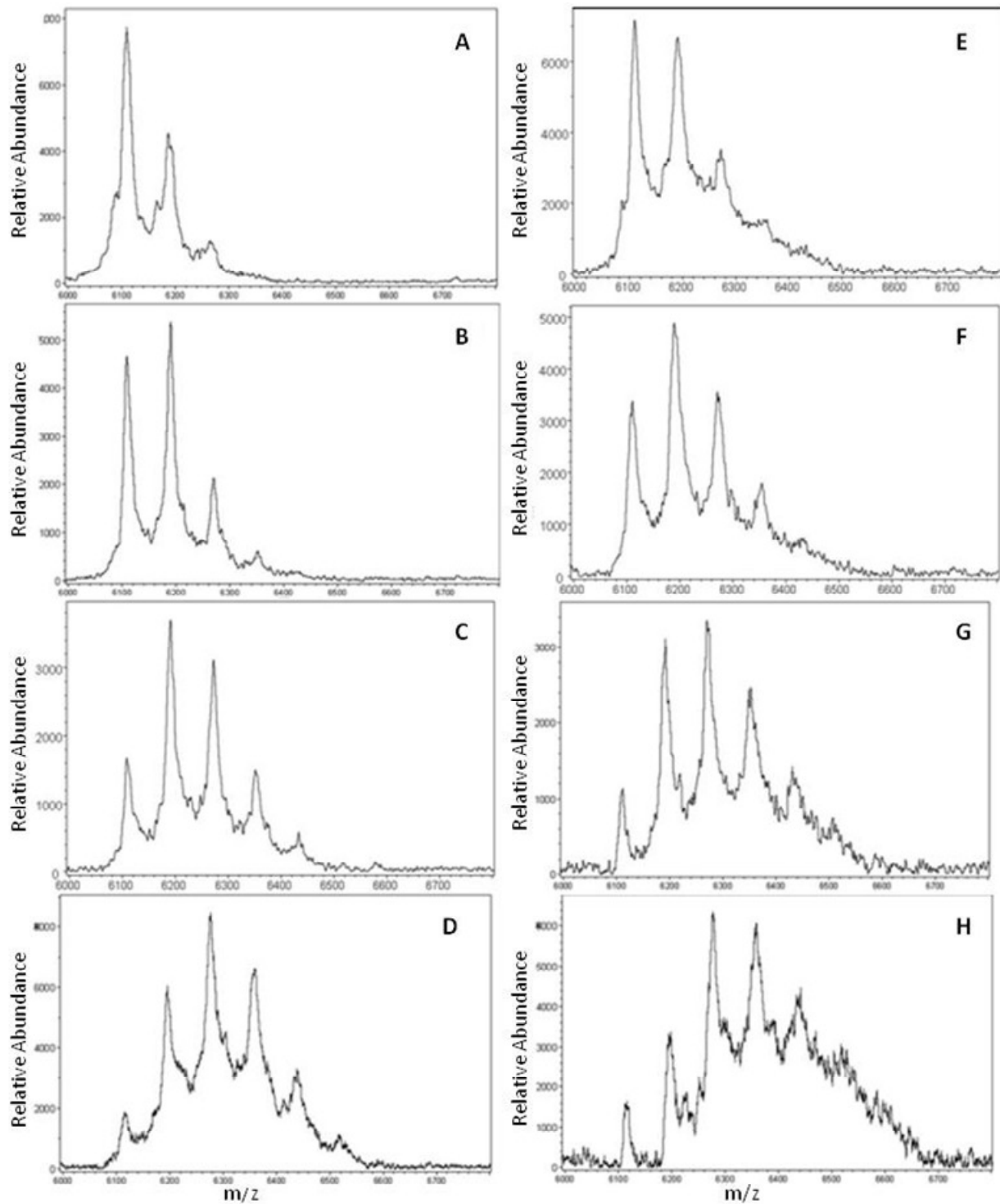


Figure 1.5. MALDI-TOF mass spectra of the +2 ion of bovine Cyt c incubated at 37°C in the presence of D-galactose for 2 days (A), 4 days (B), 7 days (C), and 11 days (D). Bovine cytochrome c incubated at 37°C in the presence of D-galactose and carnosine for 2 days (E), 4 days (F), 7 days (G), and 11 days (H).

Experimental Methods:

Preparation of Carnosine Affinity Beads:

Carnosine affinity beads were produced by attaching carnosine to benzyloxybenzylbromide resins (Advanced ChemTech) through its N-terminus following the manufacturer's protocol. We spent some time optimizing all of the experimental conditions in order to produce the best quality affinity beads possible. Briefly, the resin beads were swelled in dichloromethane (DCM) for an h and then washed 3X with dimethylformamide (DMF). 17 mg carnosine was then dissolved into 200 μ L of DMF and added to the resin. This was allowed to stir overnight at room temperature. A NP-40 lysis buffer composed of 50 mM Tris-HCl at pH 8.0, 150 mM NaCl and 1% NP-40 was prepared. The resin was washed three times with DMF, three times with DCM and three times with the lysis buffer. The same process was repeated for the pre-clear beads without the addition of carnosine.

Beads were also created with a similar method for connecting via the C-terminus, though results of the experiment were inconclusive.

Later trials involved the preparation of NHS Magnetic carnosine affinity beads through covalently binding carnosine to NHS magnetic beads (PureProteome) via its N-terminus following the manufacturer's protocol. Briefly, 200 μ g of carnosine was dissolved into 60 μ L of phosphate buffered saline (PBS). Sixty μ L of the 20% bead slurry was removed and added to a separate 1.5 mL microcentrifuge tube. This was placed into the magnetic stand and the beads were allowed to migrate to the magnet where the storage buffer was removed. Immediately, 500 μ L of ice-cold equilibration buffer was added to the beads. This buffer was a 50/50 solution of distilled water and HCl. The beads were then vortexed rigorously and placed back into the stand

where the solution was removed. Next, the carnosine solution was added to the beads and the tube was removed from the stand. The beads were then incubated with continuous mixing at room temperature for 4 h. Afterwards the beads were placed in the magnetic stand and allowed to migrate to the magnet before the unbound C-Peptide solution was kept back for analysis. Five hundred μL of the Quench Buffer (100 mM Tris-HCl, 150 mM NaCl, pH 8.0) was added and vortexed rigorously for 30 s. The beads were placed back into the stand and the solution was removed. This process was repeated another four times. A final 500 μL of the Quench buffer is added then allowed to incubate with the beads at room temperature with continuous mixing for 1 h. Afterwards, the beads are placed in the stand, the quench buffer is removed and the beads are stored in 100 μL of PBS. The process was repeated for the pre-clear beads without addition of carnosine.

Tissue Lysis:

For the initial experiments, we isolated proteins from two types of bovine tissues, specifically: heart and kidney. There were three trials for this initial experiment. The first two used tissue from bovine heart, and the last trial from bovine kidney. Bovine tissue was lysed using CelLytic MT mammalian tissue lysis buffer (Sigma) following the manufacturer's protocol. Protease inhibitors were added to the lysis buffer. Briefly, the tissue was homogenized in lysis buffer and allowed to sit on ice for 30 min to ensure optimal lysis of the tissue. The tissue lysate was then centrifuged at 12,000 G for 15 min at 4°C, and the supernatant lysate was transferred to a clean microcentrifuge tube. Uncoupled benzyloxybenzylbromide beads were added to the lysate to pre-clear the lysate of any proteins that would have an affinity for the beads themselves.

The later experiments with magnetic beads involved the lysis of bovine kidney, first, then later the use of lean Zucker rat plasma.

Protein Isolation:

Proteins capable of binding to carnosine and/or heme-chelated carnosine were isolated using the affinity beads created above. We optimized all experimental conditions (time, temperature, etc.) until we were able to isolate proteins from different tissue lysates. Briefly, pre-cleared lysates were incubated with carnosine affinity beads overnight at 4 °C. After the reaction was complete, the supernatant was removed, and the beads were washed 3X with phosphate buffered saline (PBS).

SDS PAGE Analysis of Isolated Proteins:

Proteins isolated from the affinity columns were separated by sodium dodecyl sulfate-polyacrylamide gel electrophoresis (SDS-PAGE) prior to mass spectrometric analysis. Proteins were eluted from the affinity beads with the addition of SDS-PAGE sample loading buffer and loaded directly onto the PAGE TGX™ gels (4-15% gels, BioRad). Briefly, proteins were separated for 30 min at 200V using Tris/Glycine/SDS running buffer. DTT (0.1 M) was added directly to the samples, and all samples were heated for 5 min at 100°C prior to gel loading. Proteins were visualized with Bio-Safe Coomassie Stain (Bio-Rad).

Preparation of Tryptic Digests of Protein Samples from SDS-PAGE Bands:

Protein bands were excised, reduced with DTT, treated with iodoacetamide, and digested with trypsin overnight at room temperature following the procedure at <http://ms-facility.ucsf.edu/ingel.html>.

Briefly, protein bands were excised from gel, diced into smaller pieces and placed in .5 mL siliconized tubes. 100 µL of 25 mM NH₄HCO₃/50% ACN was added to the gel pieces and

vortexed for 10 min. A gel loading tip was used to extract the supernatant that was discarded. This was repeated twice more until the gel pieces no longer contained visible staining. Next, a fresh solution of 10 mM DTT in 25 mM NH_4HCO_3 was prepared. About 25 μL of DTT was added to each tube. They were vortexed and spun briefly before being allowed to incubate at 56° C for 1 h. Then the supernatant was removed and discarded and 30 μL of a freshly prepared 55 mM iodoacetamide in 25 mM NH_4HCO_3 was added to the gel pieces. These were allowed to incubate in the dark for 45 min. The supernatant was then removed, and 100 μL of NH_4HCO_3 was added to wash the gels and was then removed. Next, the gels were washed twice with 100 μL of 25 mM NH_4HCO_3 /50% acetonitrile (ACN) . All supernatant was removed. Then, a solution containing 0.2 μg trypsin in 30 μL of 25 mM NH_4HCO_3 was added to each gel piece and allowed to digest over night. The digest solution was transferred into a clean siliconized tube, and to the gel pieces, 30 μL of 50% ACN/5% formic acid was added, and vortexed for 30 min. These were then spun down and sonicated. The solution was removed and the digest solution was added. The process was then repeated once more. The resulting digest solution was then placed into a centrifugal evaporator where the solutions were reduced to a volume of 10 μL .

Analysis of Tryptic Digests of Proteins by MALDI-TOF Mass Spectrometry:

The tryptic digests of the proteins were purified with C_{18} ZipTips (Millipore) and analyzed on a Bruker Autoflex MALDI-TOF mass spectrometer (Billerica, MA). Prior to analysis, the peptide preparations (0.6 μL) were each mixed with a 50% aqueous acetonitrile solution (0.6 μL) of saturated α -cyano-4-hydroxy-cinnamic acid containing 0.05% TFA as matrix, spotted onto a stainless steel sample plate and allowed to air dry. The mass spectra were recorded in positive ion mode with a 60 nsec delay in the m/z range from 500 to 3500.

Typically, 500 spectra will be accumulated with 50 laser shots for each sample spot analyzed. The resulting peptide mass fingerprint spectra obtained for each protein analyzed was used to identify the protein by inputting the peptide molecular weights obtained into the mascot search engine.¹⁹

Analysis of Tryptic Peptide Amino Acid Sequences by LC/ESI/MS:

The tryptic digests of the proteins were purified with C₁₈ ZipTips (Millipore) and analyzed on a ThermoFinnigan LCQ mass spectrometer. The tryptic peptides were fractionated on 10µm spherical C₁₈ resins and eluted directly into the electrospray source of a ThermoFinnigan LCQ mass spectrometer equipped with a quadrupole ion trap mass analyzer. The reverse phase microcapillary columns were constructed according to a procedure modified from Kennedy and Jorgensen.²⁰ The loading of peptides onto the columns was performed using a helium bomb. Once applied to the columns, the peptides were first washed with 0.1% acetic acid for 3 min and were then collectively eluted from the columns with 60% acetonitrile in 0.1% acetic acid at a flow rate of 2 µL/min using the helium bomb. The column elutes directed into the electrospray source were analyzed by MS and tandem mass spectrometry (CID fragmentation with He) favoring isolation and fragmentation of doubly charged ions.

The ESI/MS system was operated with the Xcalibur software (version 2.0, ThermoFinnigan), with the same software used also for data analysis. The mass spectrometer was set to function in the positive ion mode with parameters optimized during direct infusion of peptide standards with solvent. The solvent, consisting of 50/50 (v/v) 0.1% acetic acid in water/acetonitrile, was applied at a flow rate of 3 µL/min. Nitrogen was used as the sheath gas (setting at 60), and ultrapure helium was used as the collision gas. The ion spray voltage was set as 4.5 kV and the capillary temperature was 210°C.

Determining the Effect of Carnosine on AGE Structure Formation:

Glycated cytochrome C was prepared by incubating 1 mg of bovine cyt c with 35 mg of D-galactose in 250 µL of PBS, pH 7.4 at 55⁰C for 3 h. After incubation, an Ultracel YM-33 kDa

cutoff filter was used to remove excess galactose from the sample prior to further analysis. The sample was diluted to a volume of 250 μL with PBS and 125 μL of sample was transferred to a new microcentrifuge tube. Carnosine was added to one sample at a final concentration of 10 mM, and both samples were diluted to 500 μL with PBS and allowed to incubate at 37⁰C for up to 42 days.

Sodium Borohydride Reduction:

A freshly prepared 100 mM solution of sodium borohydride in 0.02N NaOH was immediately reacted 1:1 with each of the cytochrome c protein preparations. Incubations were allowed to proceed at room temperature for 1h, and reactions were terminated by 1N HCl (1:12.5 vol/vol). Following the addition of HCl to samples, mixtures were incubated at room temperature for 5 min. The pH of samples was then adjusted to physiological pH by a 1:1 dilution with a 100 mM Tris buffer, pH 7.5.

UV-VIS absorbance profile of hemin:

Hemin was added to a saturated solution of carnosine in PBS at pH 7.4. After 30 min, absorbance spectra were measured on a Cary 50 Scan UV-Visible spectrophotometer.

Results and Discussion:

Identification of Carnosine Binding Proteins Isolated from Bovine Kidney Tissue:

Carnosine is a rather simple dipeptide that could act as a signal or cofactor for cellular processes in the body. Little is known as of yet about the biological function of this dipeptide. Knowledge gained from previous studies in the Frost lab showed that carnosine acts on heme possibly via chelation of the iron atom in the heme to the His residue of carnosine. This experiment was designed to gain a better understanding of how carnosine acts in the body by examining what proteins an affinity column with carnosine attached would pull out of cell lysates. By knowing the proteins, inferences can be made as to how carnosine works with these known proteins in the body.

The basic protocol for this experiment is summarized in Figure 1.6. We developed carnosine affinity beads by attaching carnosine to benzyloxybenzylbromide resins via the peptide's N-terminus. We then lysed bovine kidney tissue and incubated the cellular lysates with the affinity beads overnight at 4 °C (lysates were pre-cleared with uncoupled benzyloxybenzylbromide resin beads). Proteins isolated with the affinity beads were separated by reducing SDS-PAGE, digested with trypsin, and analyzed by MALDI-TOF mass spectrometry. The SDS-PAGE gel is shown in Figure 1.6. Lane 1 of the gel contained molecular weight markers from which we could obtain approximate molecular weight values for the proteins isolated from the beads. Lane 2 contained bovine kidney lysate. This lane is the darkest because it contains all of the proteins extractable in the lysate. Lane 3 was left blank, and lane 4 contained proteins isolated from bovine kidney tissue lysates. Several Protein bands appeared, but three at approximately 150 kDa, 60 kDa, and 37 kDa (labeled in figure 1.7) were further analyzed by mass spectrometry.

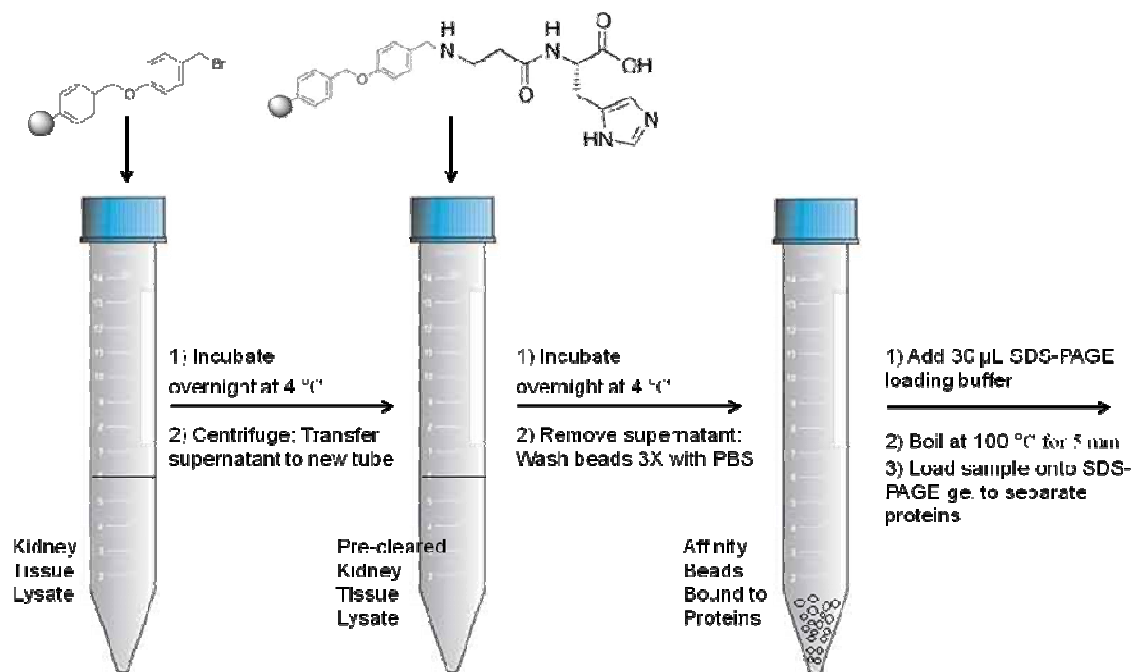


Figure 1.6. Basic experimental protocol for protein isolation using the carnosine affinity beads.

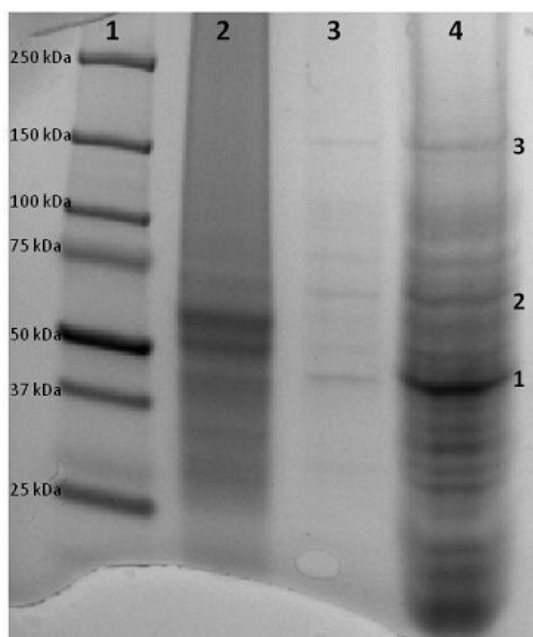


Figure 1.7. SDS-PAGE gel separation of proteins. Lanes: 1) molecular weight markers, 2) kidney cell lysate, 3) “blank”, 4) proteins eluted from kidney cell lysate using carnosine beads. Protein bands 1, 2, and 3 were excised from the gel for further analysis.

The proteins in bands 1, 2, and 3 from the SDS-PAGE gel were identified by mass spectrometry through the technique of Peptide Mass Fingerprinting (PMF). In PMF, an unknown protein is cleaved into smaller peptide fragments using a specific protease, most commonly trypsin. The molecular weight of each fragment peptide is then accurately measured by mass spectrometry. These peptide masses are then compared to a computer database of known protein sequences. Mascot, a computer program, works to take the unknown sequence from the database and compares them with the masses in order to determine a protein match. In this experiment, the proteins isolated were identified via excising a protein band from the gel, digesting the protein with trypsin, and analyzing the resulting peptide fragments with MALDI-TOF mass spectrometry.

We were able to successfully identify several putative carnosine-binding proteins from bovine kidney tissue using our carnosine affinity beads (Table 1. 2). The MALDI-TOF mass spectrum generated from the tryptic digest of the protein at about 37 kDa in lane 4 of the SDS-PAGE gel (marked as 1 in figure 1.7) is shown in Figure 1.8. This protein was identified as haptoglobin. Haptoglobin (Hp) is a protein involved in the removal of free hemoglobin from plasma (Figure 1.9). Hp is an acute phase protein whose transcription is increased in response to inflammatory stimuli. Hp functions to bind to free hemoglobin in the plasma. From here, the hemoglobin can be degraded by enzymes instead of going to the kidney, preventing iron loss and kidney damage by the hemoglobin.²¹ The protein is produced primarily in hepatocytes, as well as in other tissues such as epithelial, lung and kidney tissues. Carnosine could be chelating to the heme group of hemoglobin and assisting in the heme detoxification process.

Table 1. 2. Carnosine-binding proteins identified by mass spectrometry.

Protein	Description
Actin	A ubiquitous protein involved in the formation of filaments that are a major component of the cytoskeleton.
T-Complex Protein 1	Molecular chaperone; assists the folding of proteins upon ATP hydrolysis; known to play a role, in vitro, in the folding of actin and tubulin.
Haptoglobin	Binds free hemoglobin in plasma and inhibits the oxidative activity of its heme group; has a protective influence on the hemolytic kidney.

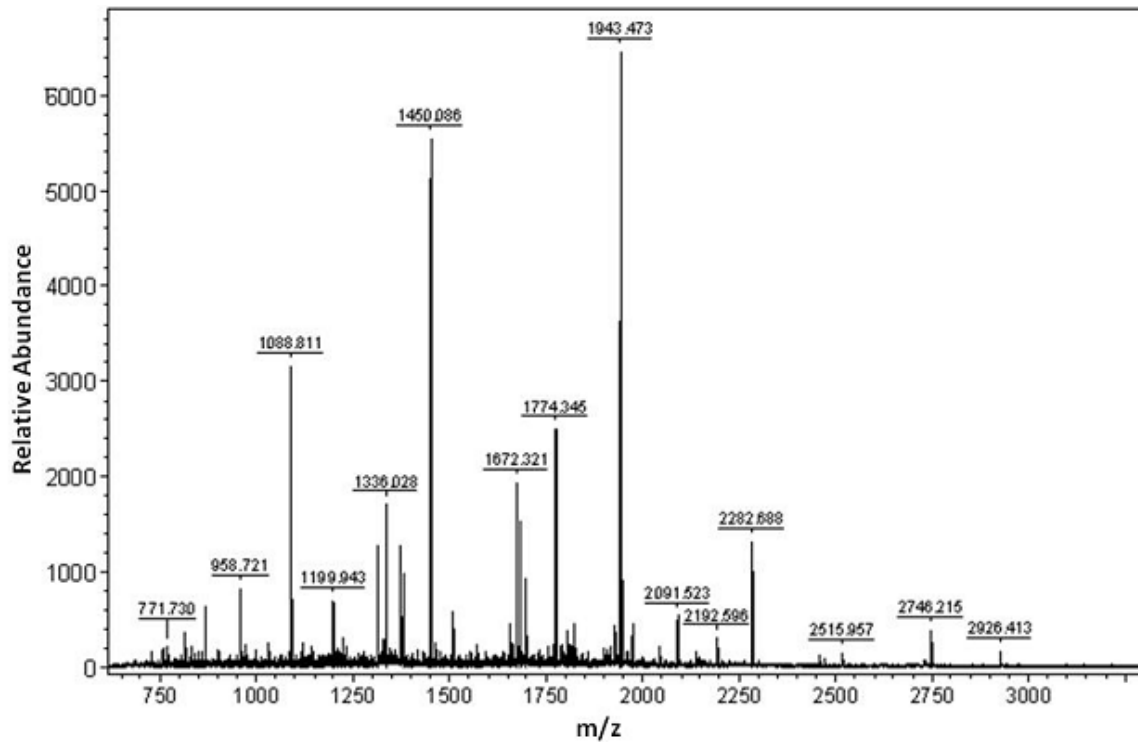


Figure 1.8. MALDI-TOF peptide fingerprint mass spectrum for the protein excised from band 1 of the SDS-PAGE gel (Figure 5).

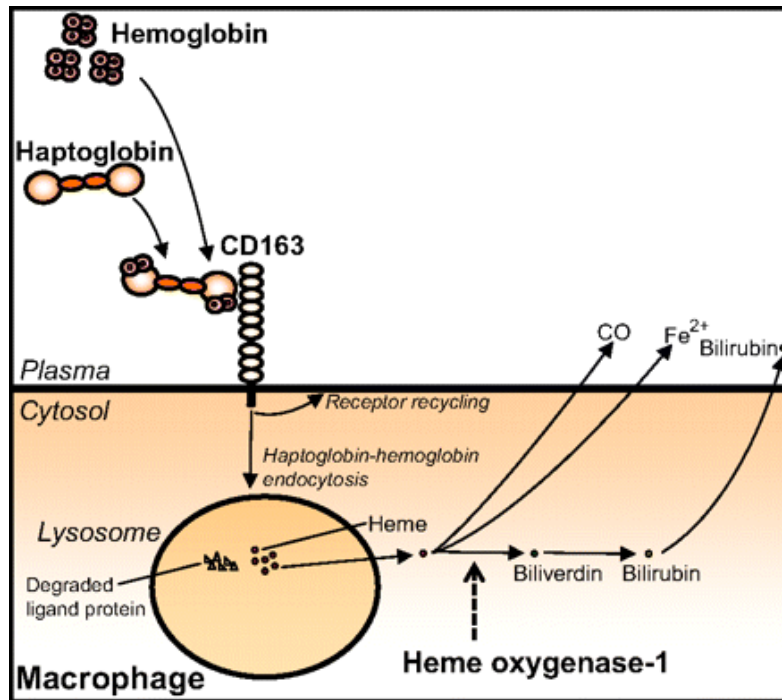


Figure 1.9. Binding of haptoglobin to hemoglobin and uptake of the complex by the CD163 receptor expressed on macrophages.²²

The MALDI-TOF mass spectrum generated from the tryptic digest of the protein at about 60 kDa in lane 4 of the SDS-PAGE gel (marked as 2 in figure 1.7) is shown in Figure 1.10. This protein was identified as the alpha subunit of T-complex protein 1 (TCP-1). This mass spectrum also contained peptide peaks from actin. TCP-1 is a 1-MDa oligomer that is built by two rings comprising eight different 60-kDa subunits that functions to push polypeptides through it using the energy of ATP hydrolysis to fold the proteins (Figure 1.11).²³ TCP-1 is a chaperonin that regulates the folding of important proteins including actin, α -tubulin and β -tubulin. Proteins may misfold or unfold in the face of certain stresses, such as changes in the cellular environment due to ageing, temperature fluctuations, or reactive oxygen species. Chaperonins act as essential modulators of protein homeostasis to minimize aberrantly folded species by promoting their productive folding or degradation. Carnosine could be chelating to the heme group in partially

unfolded heme proteins and delivering them to the TCP-1 complex for refolding through its interaction with the alpha subunit.

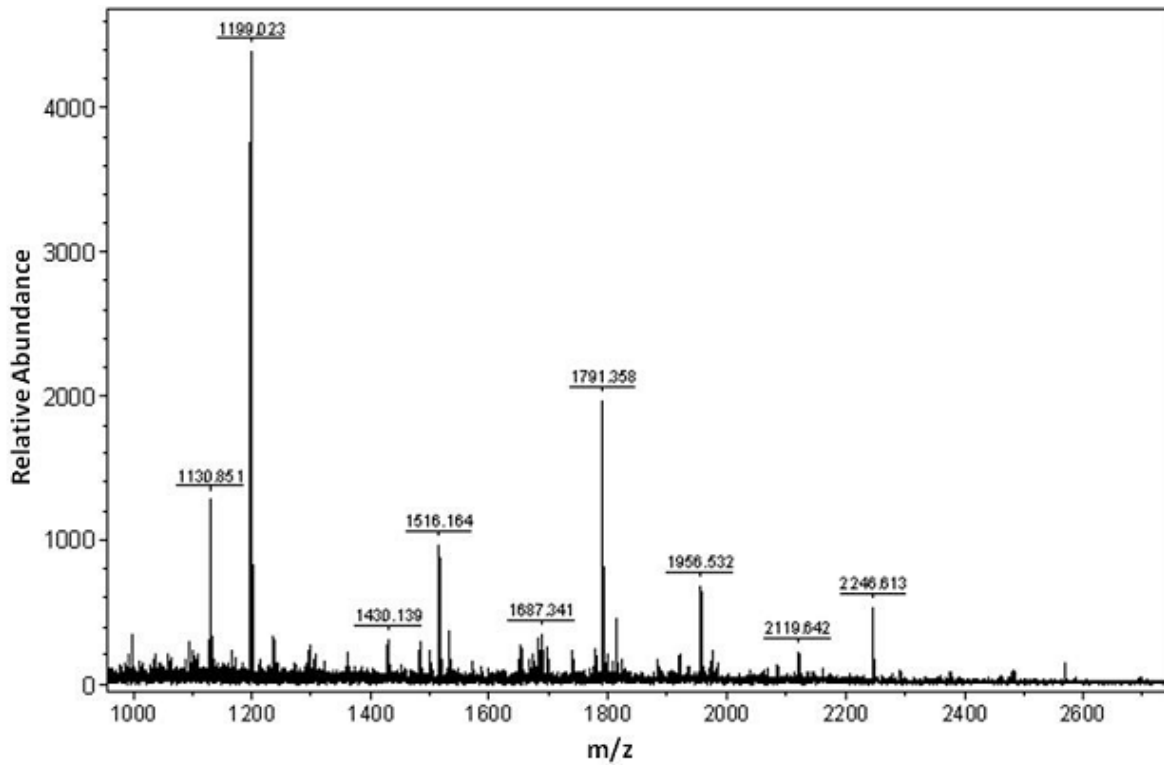


Figure 1.10. MALDI-TOF peptide fingerprint mass spectrum for the protein excised from band 2 of the SDS-PAGE gel (Figure 5).

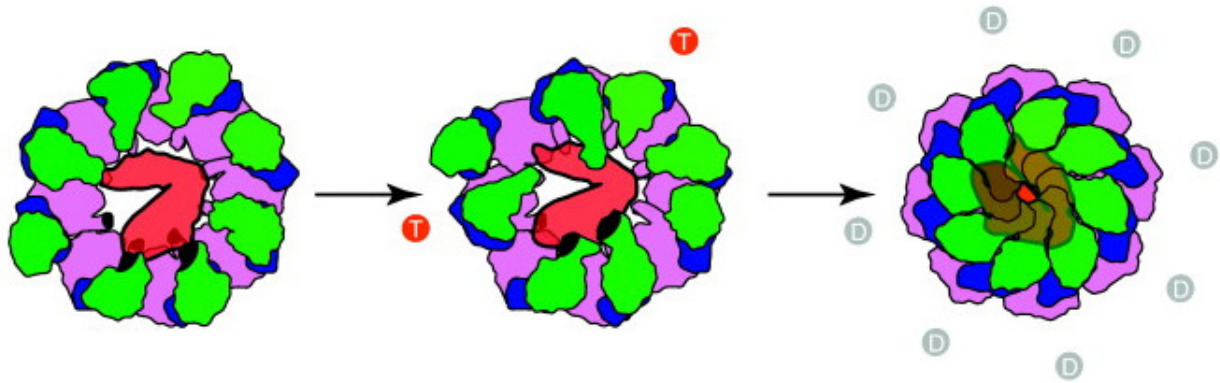


Figure 1.11. TCP-1 chaperonin with its eight different subunits, depicted in green.¹² The red T represents ATP, and the grey D represents ADP.

The MALDI-TOF mass spectrum generated from the tryptic digest of the protein at about 150 kDa in lane 4 of the SDS-PAGE gel (marked as 3 in figure 1.7) is shown in Figure 1.12. This protein was identified as actin. The protein molecular weight of 150 kDa does not correlate with the known molecular weight of actin of 45 kDa. Either the protein in this band is a polymerized trimer of the protein, or the MALDI-TOF plate contained trace amounts of a previous actin digest at this spot on the plate.

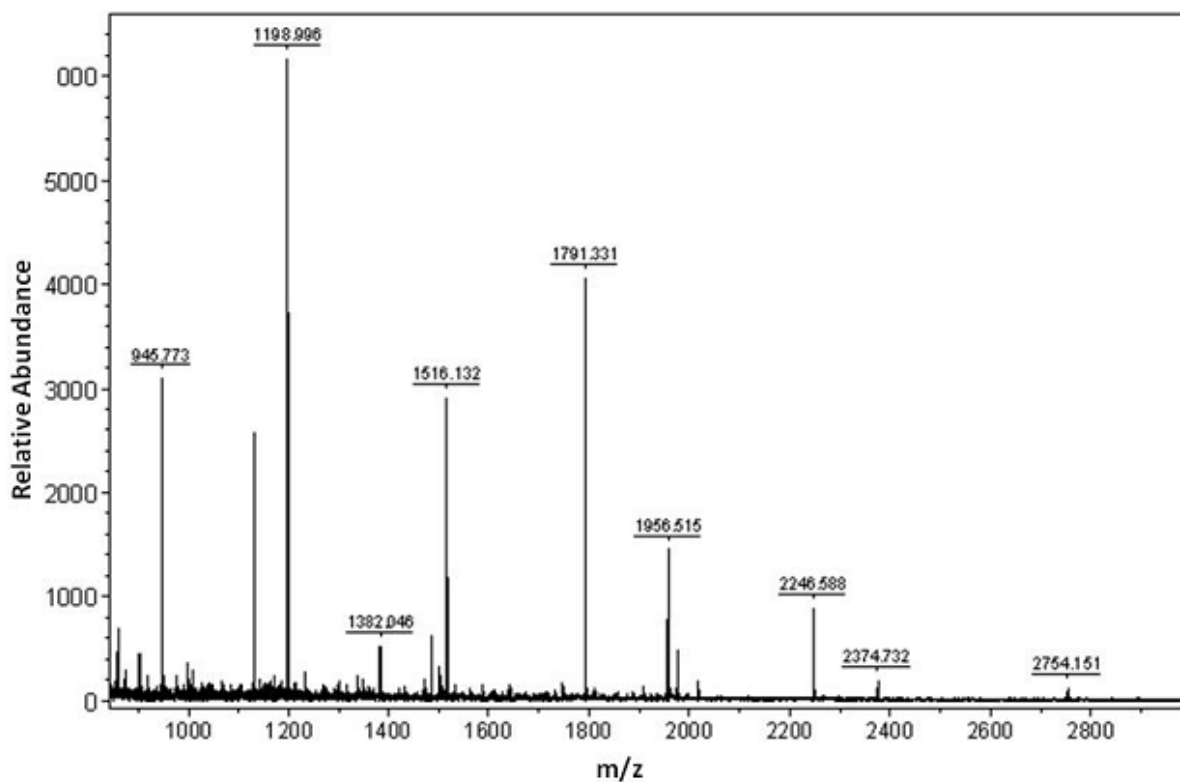


Figure 1.12. MALDI-TOF peptide fingerprint mass spectrum for the protein excised from band 3 of the SDS-PAGE gel (Figure 1.5).

Identification of Carnosine Binding Proteins Isolated from Mouse Kidney Tissue:

We repeated this experiment using a different type of beads and using a tissue lysate obtained from bovine kidney tissues and later rat plasma. We developed affinity beads by attaching carnosine to NHS magnetic beads via the peptide's N-terminus.

The NHS carnosine affinity beads identified haptoglobin again in both the plasma and the tissue, but none of the other proteins found in the bromophenoxy resin trials were identified. There were bands in the gel that could have corresponded to these proteins, but they could not be identified.

Additionally, the beta subunit of hemoglobin (HBB) was found multiple times in both the bovine kidney tissue and in the rat blood plasma. The peptide mass fingerprint spectrum from one of the Bovine Kidney trials can be found in figure 1.13. This finding is particularly interesting because it ties in with the binding of carnosine with the iron in the heme. HBB has a molecular weight of about 15.9 kDa. Its structure can be seen in Figure 1.14. HBB is involved in oxygen transport and is only found in red blood cells. It is a globular protein that forms a heterotetramer, along with a second HBB and two alpha hemoglobin subunits (figure 1.15)²⁶. Carnosine's ability to bind with HBB helps to confirm the possible interactions of carnosine with heme-containing proteins. Postulations could be that carnosine can bind to HBB so that it can more easily bind to the iron atom in the heme when necessary. Carnosine's ability to bind to HBB could also directly tie in with haptoglobin's binding to hemoglobin. Perhaps the common binding partner assists both.

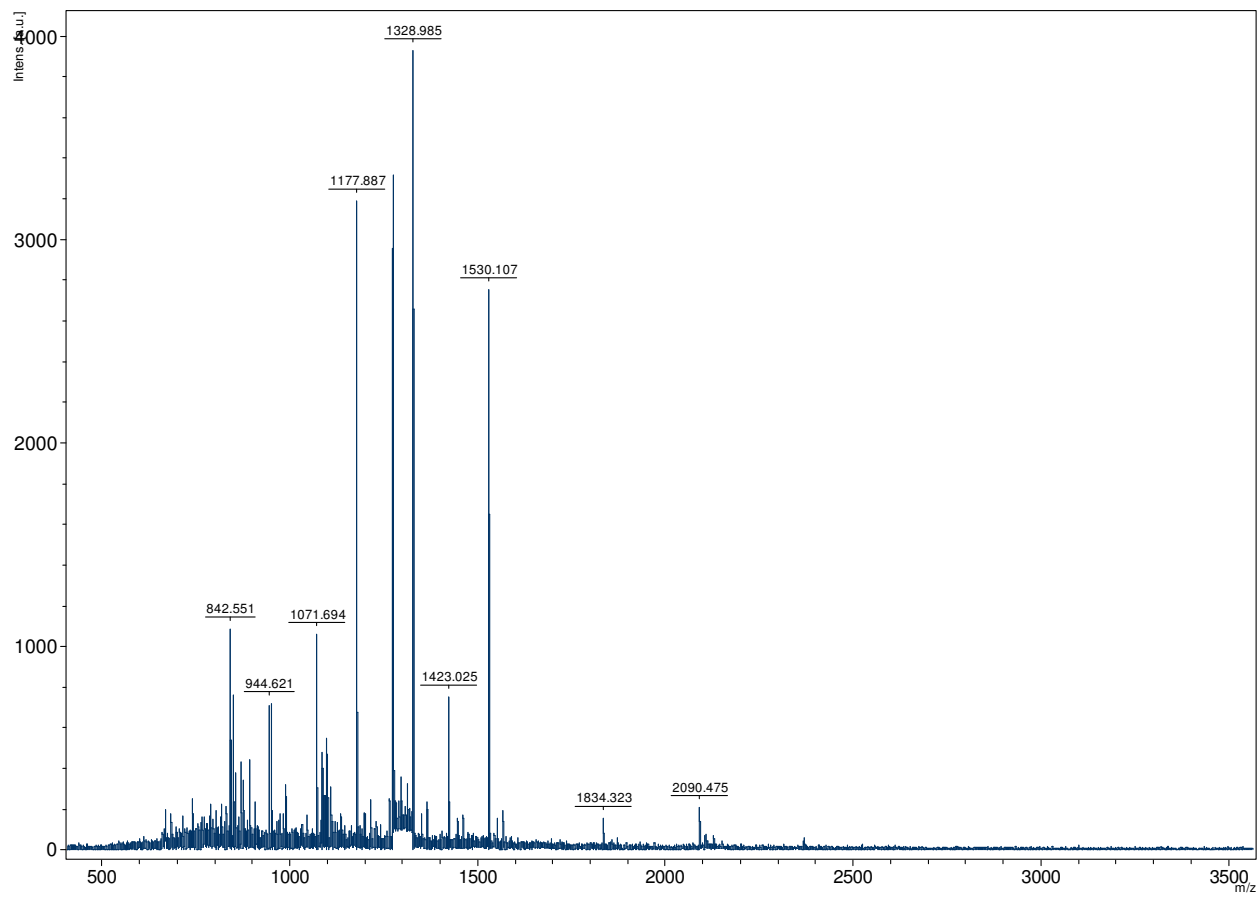


Figure 1.13. The Peptide Mass Fingerprint spectra for a bovine kidney trial using the Magnetic beads. Excised from approximately 20 kDa.

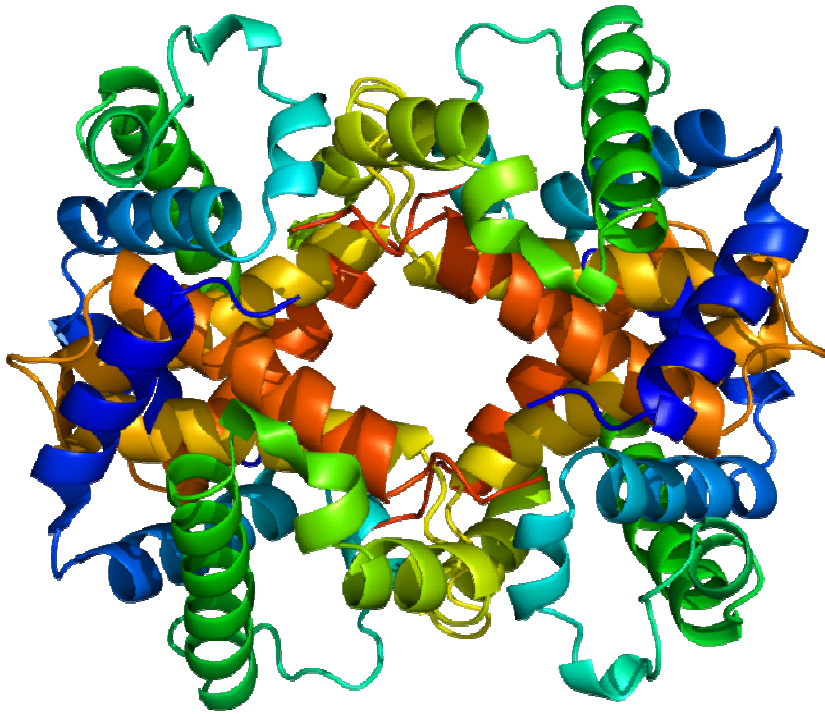


Figure 1.14. The structure of HBB based on PyMOL rendering of PDB.

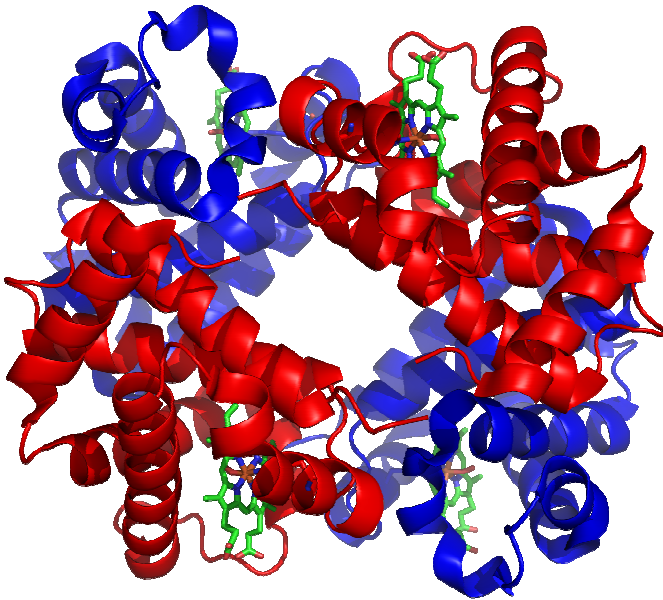


Figure 1.15. The structure of the hemoglobin heterotetramer including the four heme groups. Red represents the alpha subunit and blue represents the beta subunit. Based on a PyMol rendering of PDB.

Effect of Carnosine on the Formation of AGEs:

In order to study the effect of carnosine on the formation of AGEs, we initially incubated cyt c with galactose for 3 h at 55°C. The sugar was then removed, and the remaining protein solution was split into two equal portions. Carnosine was added to one sample to a final concentration of 10 mM, and both samples were diluted to equal volumes with buffer. The samples were then incubated at 37°C for 42 days. Aliquots of protein were removed periodically and analyzed by MALDI-TOF mass spectrometry. The resultant mass spectra for the protein samples after 42 days of incubation can be seen in Figure 1.16. The glycated cytochrome c that was not incubated with carnosine (Figure 1.16A) has a more prominent peak in the spectra at about m/z 6140 (indicated by the arrow) than when the protein was incubated in the presence of carnosine. This peak had a mass that was about 58 Da greater than the mass of the unmodified protein that would indicate the formation of an AGE structure. These results suggest that carnosine can slow down or inhibit the formation of AGE structures that can form after the initial glycation of the protein.

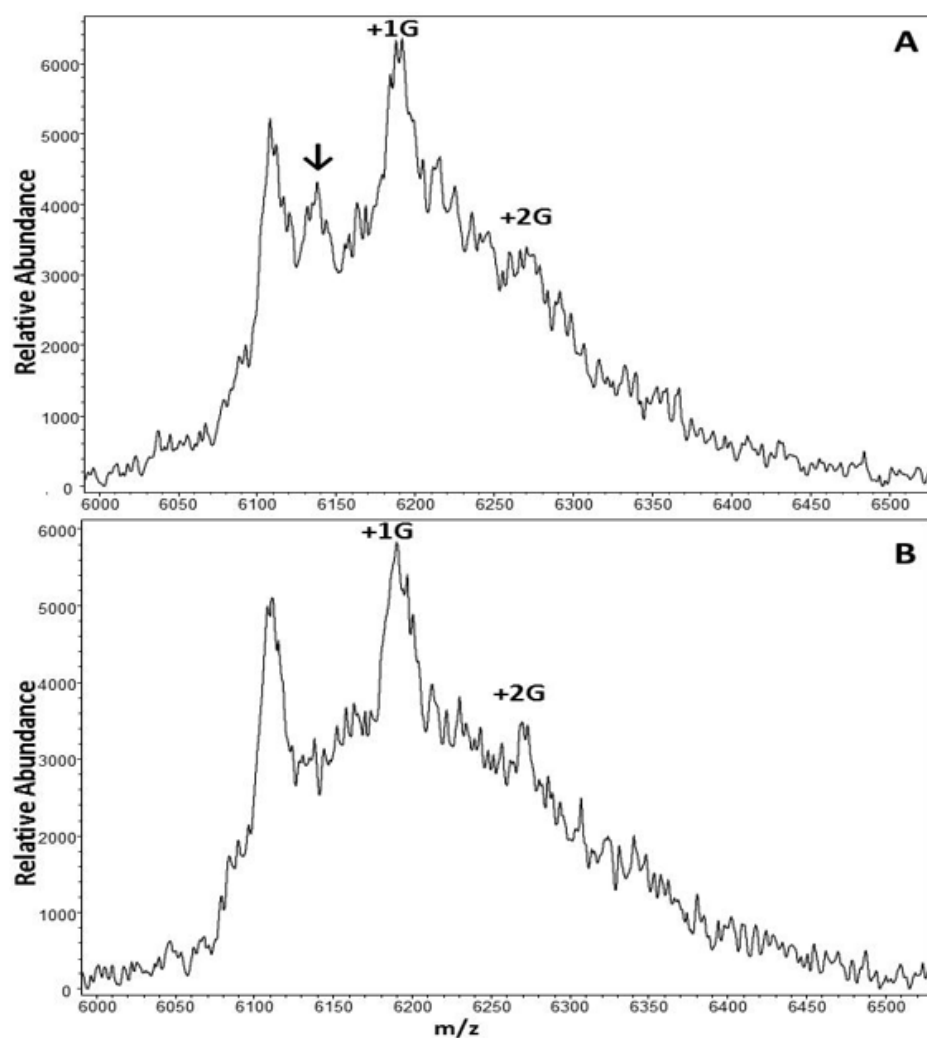


Figure 1.16. MALDI-TOF mass spectra of the +2 ion of glycosylated cytochrome c incubated at 37⁰C in the absence of carnosine (A) and in the presence of carnosine (B) for 42 days.

To investigate this further, the glycosylated proteins incubated with and without carnosine for 42 days were reduced with NaBH₄ and separately reacted with trypsin. The tryptic digest from each was analyzed by MALDI-TOF mass spectrometry in order to determine the glycation sites. The resultant peptide mass fingerprint spectra can be seen in Figure 1.17. The mass region between 2230 Da and 2430 Da was expanded and is displayed in Figure 1.18.

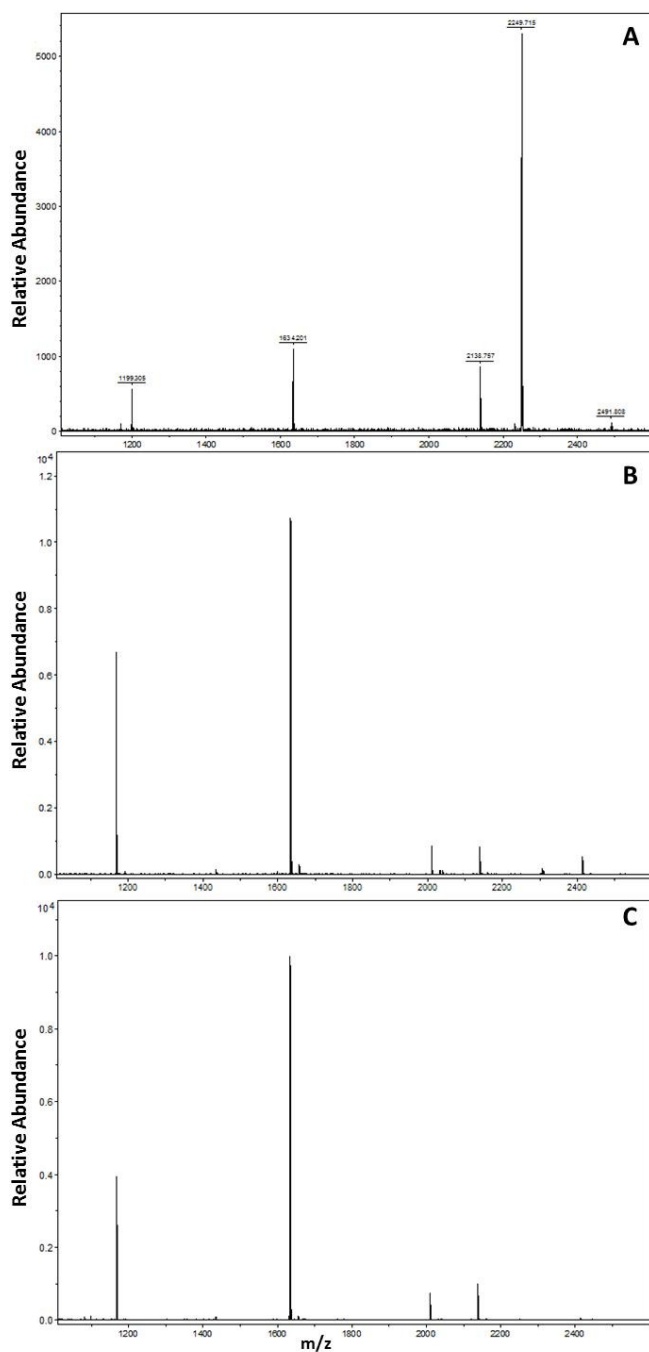


Figure 1.17. MALDI-TOF tryptic peptide mass fingerprint spectra of cytochrome C incubated at 55°C for 3 h in the absence of sugar (A), and glycosylated cytochrome C incubated at 37°C for 42 days in the absence of carnosine (B) and in the presence of carnosine (C). All protein samples were reduced with sodium borohydride prior to tryptic digestion.

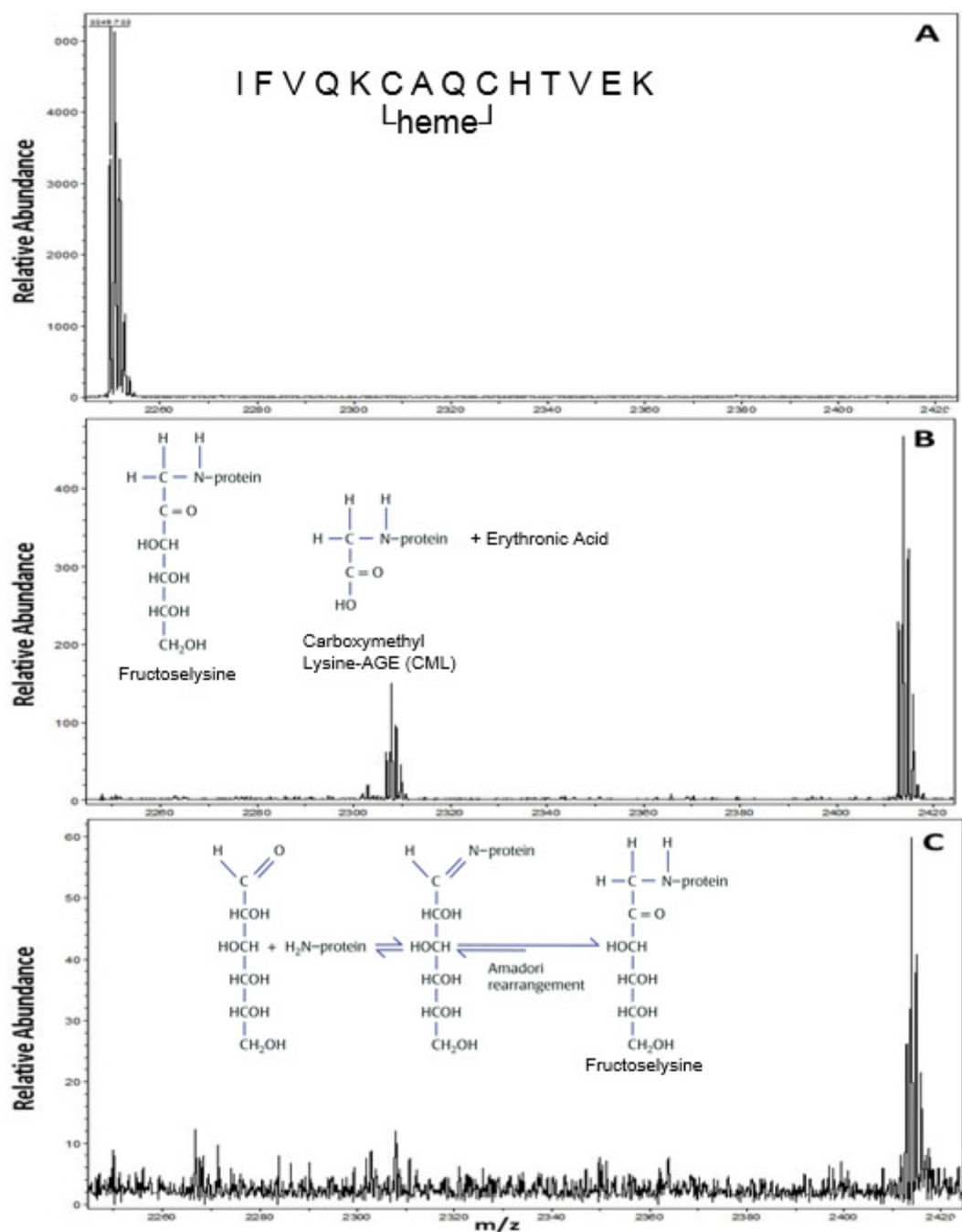


Figure 1.18. MALDI-TOF tryptic peptide mass fingerprint spectra of cytochrome C incubated at 55°C for 3 h in the absence of sugar (A), and glycated cytochrome C incubated at 37°C for 42 days in the absence of carnosine (B) and in the presence of carnosine (C). All protein samples were reduced with sodium borohydride prior to tryptic digestion.

The amino acids Lys-13, 25, 72, and 88 have previously been identified as preferred glycation sites when cyt c was incubated with D-galactose. The presence of 10 mM carnosine

was shown to inhibit the formation of AGE structures on glycosylated cytochrome c (Figure 1.16). In particular, glycosylated Lys-13 ($\Delta 164$ amu when reduced with NaBH_4) was not converted to the AGE structure ($\Delta 58$ amu) when carnosine was added to the incubation mixture (Figure 1.18). The identification of the modified lysine groups was confirmed by CAD mass spectra of the peptides at m/z 2307 and 2413. Lys-13 is located right next to the heme group in cytochrome c (Figure 1.19). We propose that the heme group facilitates the conversion of the glycosylated lysine residue into the AGE structure. The carnosine may be associating with the heme group keeping it in its reduced form (Fe^{+2}).

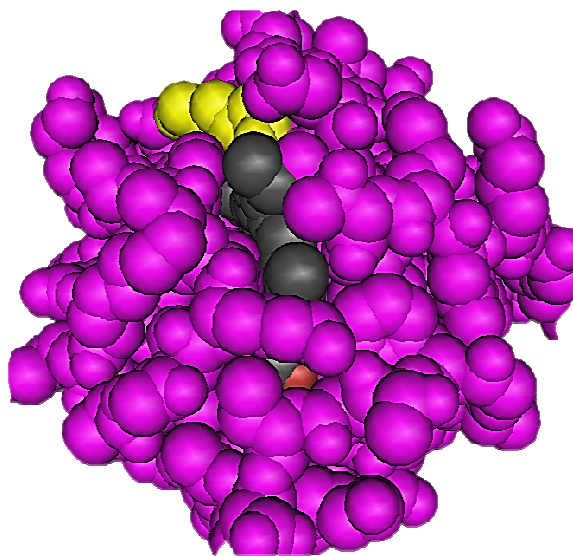


Figure 1.19. Space-filling plot of the horse cytochrome c structure. Modified lysine residue is shown in yellow and heme group is shown in grey. Adapted from the high-resolution 3-D structure of horse cytochrome c²⁴ available at the Protein Data Bank PDB ID:1HRC.

Analysis of Carnosine-Hemin Interactions:

The results from the previous experiments indicate that carnosine interacts with heme groups. Carnosine contains a histidine group as part of its structure, and histidines are known to ligate to the Fe ion in heme groups. In fact, heme is attached to the proteins hemoglobin and myoglobin through a ligand interaction between the Fe atom and a proximal histidine residue located in the heme-binding site. Hemin is protoporphyrin IX (heme B) containing a ferric iron ion (Fe^{+3}). We have found that the addition of carnosine to a solution of free hemin drastically increases the solubility of hemin and causes a shift of the λ_{max} in its UV-Vis absorbance profile. The wavelength of the Soret band maxima of hemin in PBS at pH 7.4 is 386 nm. When carnosine was added to the solution, the wavelength maxima shifted to 408 nm (Figure 1.20). In addition, the bands arising from the Q bands were shifted. This significant change in the heme active site in the presence of carnosine may correspond to a 6c low-spin Fe^{+2} state for the heme. These results suggest that the carnosine was ligating to the iron most likely through the histidine side chain. The conversion of the oxidized iron in hemin (Fe^{+3}) to the reduced (Fe^{+2}) state would be beneficial to cells because the Iron II state cannot catalyze the production of free radicals in the cell therefore preventing oxidative stress.²⁷

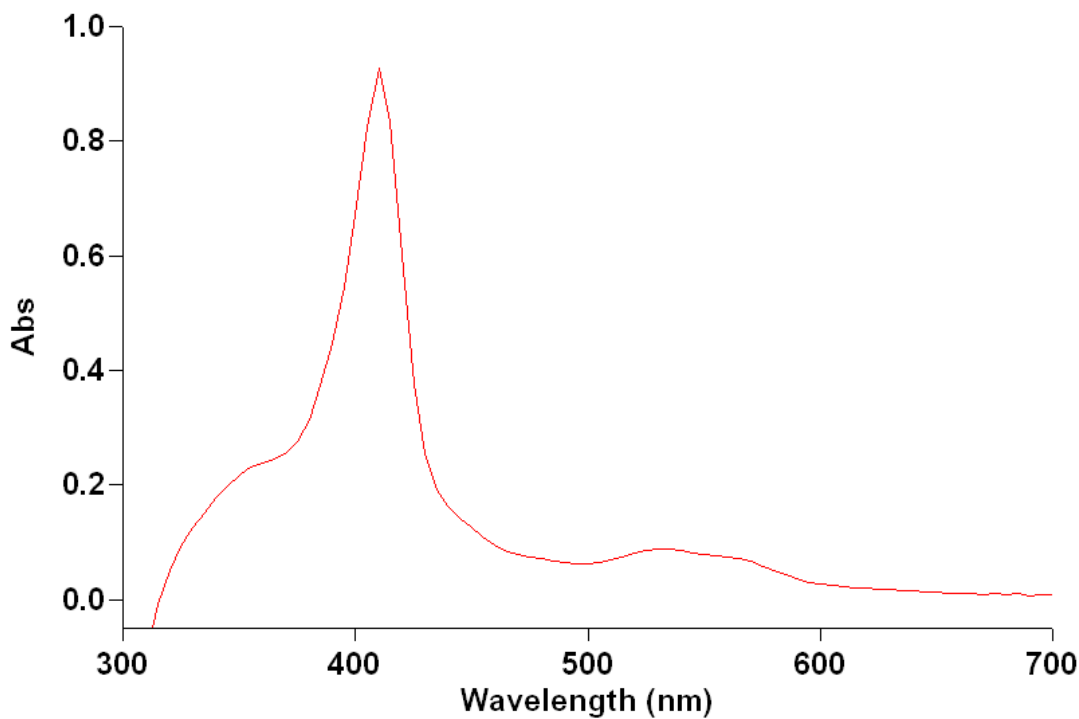


Figure 1.20. UV-VIS absorption profile of hemin in a saturated solution of carnosine. Inset is the absorption profile of hemin in PBS. The dimer absorbs at 345 nm, while the monomer absorbs at 386 nm.

Future Work

Further research could delve into the possibilities of using carnosine as a drug to prevent heme toxicity in the body. Carnosinase will degrade free carnosine in the blood stream meaning increasing the amount of carnosine in the body would likely increase degradation. To avoid this, carnosine could be derivatized so that carnosinase will not recognize it as a substrate. However, without a complete understanding of the biological function of carnosine, it would be difficult to predict how the derivatization would affect its function. In addition, this would have to be carefully regulated, because too much carnosine could cause carnosinemia in patients. Excess amounts of carnosine have been known to harm people causing various forms of neurological problems.

Because the tissue and plasma utilized in these experiments had been frozen a few years, it is possible the time could have degraded some of the protein's binding abilities. Future experiments could involve repeats of the affinity column experiment with fresher tissue samples.

References:

1. Bonfanti, L. Peretto, P., de Marchis, S., and Fasolo, A. (1999) *Prog. Neurobiol.* 59, 333-353.
2. McFarland G. A. and Holliday R. (1994) *Exp. Cell Res.* 212, 167–175.
3. McFarland G. A. and Holliday R. (1999) *Exp. Gerontol.* 34, 35–45.
4. Quinn P. R., Boldyrev A. A. and Formazuyk V. E. (1992) *Mol. Aspects Med.* 13, 379–444.
5. Hipkiss A. R., Michaelis J. and Syrris P. (1995) *FEBS Lett.* 371, 81–85.
6. Voet D., Voet J.G. and Pratt C. W. (2008) *Fundamentals of Biochemistry* Third Edition, 611.
7. Bunn H. F. and Forget B. G. (1986) *Hemoglobin: Molecular, Genetic and Clinical Aspects.*
8. Kumar, S. and Bandyopadhyay, U. (2005) *Toxicology Lett.* 157, 175-188.
9. Anzaldi L.L. and Skaar E.F. (2010) *Infect Immun.* 78, 4977-4989.
10. Jomova K., Vondrakova D., Lawson M. and Valko M. (2010) *Mol. Cell Biochem.* 345, 91-104.
11. Urbanowski, J.C., Cohenford, M.A., and Dain, J.A. (1982) *J. Biol. Chem.* 257, 111-115.
12. Armbruster, D.A. (1987) *Clin. Chem.* 33, 2153-2163.
13. Bohlender, J.M., Sybille, F., Stein, G., and Wolf, G. (2005) *C. Am. J. Physiol. Renal. Physiol.* 289, F645-F659.
14. Olufemi, S., Talwar, D., and Robb, D.A. (1987) *Clin. Chim. Acta* 163, 125-136.
15. Tessier, F.J. (2010) *Pathologie Biologie* 58, 214-219.
16. Lange, C. and Hunte, C. (2002) *Proc. Natl. Acad. Sci.* 99, 2800-2805.
17. Craig, D. and Wallace C.J. (1993) *Protein Sci.* 2, 966-976.
18. Kostrzewa, A., Pali, T., Froncisz, W. and Marsh D. (2000) *Biochemistry* 39, 6066-6074.
19. Matrix Science Ltd. (2008) MASCOT peptide mass fingerprint.
http://www.matrixscience.com/cgi/search_form.pl?FORMVER=2&SEARCH=PMF.
20. R.T. Kennedy, J.W. Jorgensen(1989) *Analyt. Chem.* 61,1128-1135.

21. Wassell J. (2000) *Clin. Lab.* 46, 547-552.
22. Nielsen, M. J. and Moestrup, S.K. (2009) *Blood* 114, 764-771.
23. Hugo Yébenes, H., Mesa, P., Muñoz, I.G., Montoya, G. and Valpuesta, J.M. (2011) *Trends Biochem. Sci.* 36, 24-432.
24. Bushnell, G.W., Louie, G.V., and Brayer, G.D. *J.Mol.Biol.* (1990) 214, 585.
25. Ito, Y. and Walter, M. (2013) *InTech* ISBN: 978-953-51-1064-4.
26. Shaanan, B. (1983). *J. Mol. Biol.* 171, 31–59.
27. Imlay, James A. (2003). *Annual Review of Microbiology* 57, 395–418.

Proinsulin C-Peptide as an Active Biomolecule

Introduction:

Proinsulin connecting peptide, or C-peptide, is part of a precursor to insulin in the insulin biosynthesis pathway. ¹ The 31 amino-acid peptide (Figure 2.1) serves to connect the A chain to the B chain in proinsulin and facilitates the correct folding of proinsulin to allow the formation of the disulfide bridges between the A-chain and the B-chain of insulin.

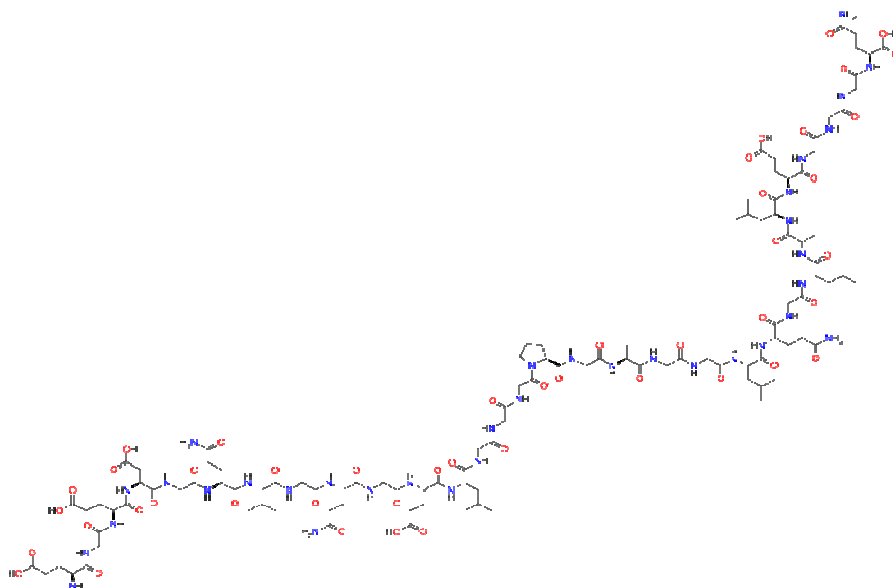


Figure 2.1. Structure of insulin C-peptide.

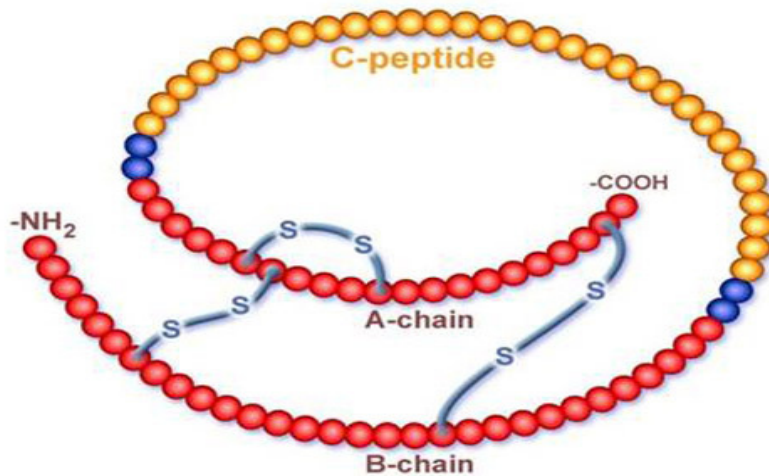


Figure 2.2. Proinsulin structure. The mature insulin peptide is shown in red and the C-peptide is shown in yellow.

Proinsulin (Figure 2.2) is formed within pancreatic β -cells. In the insulin biosynthesis pathway (figure 2.3), C-peptide is cleaved off via a trypsin-like protease located in the endoplasmic reticulum of pancreatic β -cells. C-peptide is then stored in Golgi secretory granules along with mature insulin peptide and is secreted in equimolar amounts along with insulin into the portal circulation. Although C-peptide has long been considered biologically inert, there is some evidence that it has a function within the body. C-peptide is stored in pancreatic β -cells along with insulin and released into circulation with insulin. It is used as a marker for distinguishing Type-1 diabetes from Type-2. C-peptide also has a considerably longer half-life in the body than insulin. C-peptide is cleared by the kidney and has a half-life of about 20 to 30 min compared to insulin that is cleared through the liver and has a half-life of about 3 to 5 min.²

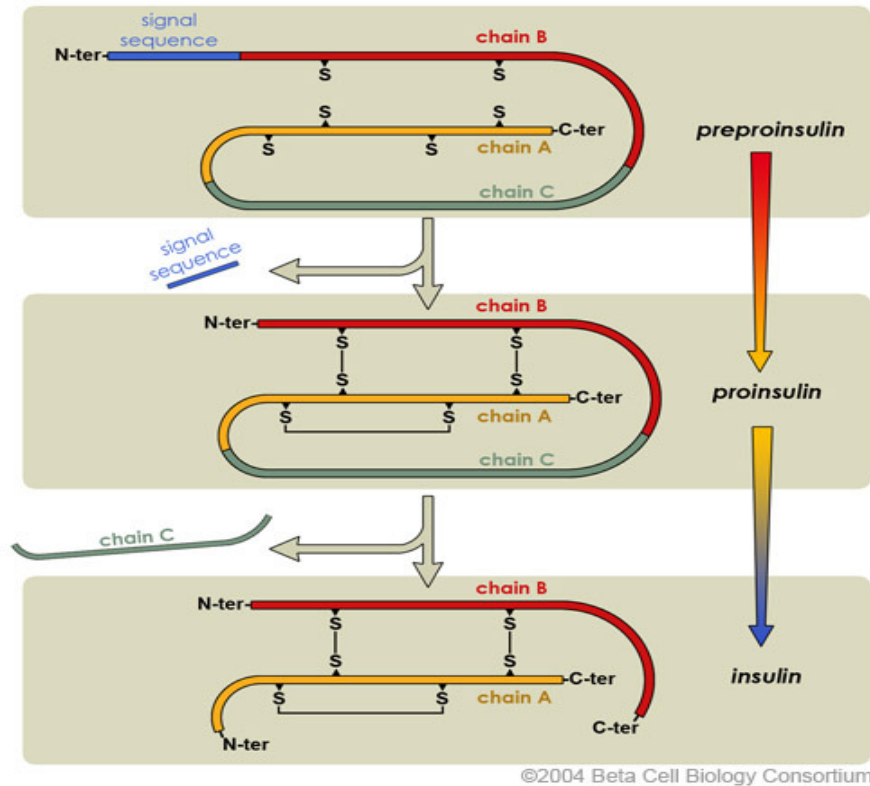


Figure 2.3. Insulin Biosynthesis Pathway as proposed in “Insulin Biosynthesis: Evidence for a Precursor”¹

C-Peptide levels are closely tied with insulin since they are created in a one to one ratio.

C-Peptide can be used as a marker of insulin production and is used to help determine the difference between a person with Type-1 diabetes and Type-2. In Type-2, more insulin and C-peptide are synthesized as where in Type-1, considerably less insulin and c-peptide is produced.

The primary difference in the diabetes types is Type-2 is associated with insulin resistance and initially has normal or elevated levels of insulin and c-peptide that can decrease over the course of the disease, and Type-1 is associated with less insulin production due to a decrease in

functional pancreatic β -cells.³ Diabetes is a group of metabolic diseases associated with high

blood glucose levels. Insulin is the primary peptide hormone associated with diabetes. It works to inhibit glucagon release and thus regulate carbohydrate and fat metabolism. Insulin binds to receptors on cells found in the liver, skeletal muscles, and fat causing glucose absorption. Insulin

is medically used to treat patients with diabetes; however, insulin treatment has been shown to lower C-peptide levels in Type-2 diabetics.⁴

Type-1 diabetes is associated with a lowered production of insulin and a loss of insulin-producing pancreatic beta cells.³ Approximately 10% of diabetics have this type. It involves sudden onset before age 40 and is considered insulin-dependent. Type-2 diabetes, on the other hand, is characterized by low insulin-sensitivity and high insulin production. Approximately 90% of diabetics have this type and it primarily affects obese adults with gradual onset. Symptoms of diabetes are numerous involving both microvascular and macrovascular complications. Microvascular issues include retinopathy (cataracts, and glaucoma in the eyes), nephropathy (microalbuminuria and kidney failure), and neuropathy (nerve damage in the peripheral nervous system). Macrovascular complications include stroke, cognitive impairment, coronary syndrome, myocardial infarction, congestive heart failure, peripheral vascular disease leading to gangrene, ulceration and amputation. Typically microvascular complications are more associated with Type-1 and macrovascular complications more with Type-2; however, some complications are shared.

Because C-peptide is synthesized in a one to one ratio with insulin, it has been suggested that it may also have a function in preventing diabetes. For this reason, and for the fact that C-peptide is not degraded immediately after the correct folding and processing of the mature insulin peptide, C-peptide has been the subject of several major studies that show a more active role in the body. C-peptide is now believed to be an important, biologically active molecule that can improve some of the complications associated with diabetes mellitus. The biological functions of C-peptide are still being heavily investigated, but the peptide is thought to exert its biological effects through both receptor-mediated and non-receptor mediated pathways.

Studies have been conducted that demonstrated beneficial effects of the C-peptide in the diabetic state, including improvements of kidney and nerve function. C-peptide has been shown to bind to membrane surfaces of cultured cells derived from human renal tubules, skin fibroblasts, and saphenous vein endothelium.^{2,5-7} The pretreatment of cells with pertussis toxin, known to modify receptor-coupled G proteins, abolished the binding, so it was concluded that the C-peptide was binding to specific G protein-coupled receptors on cell membranes.⁷ However, a C-peptide specific cell surface receptor has never been isolated or identified to date. C-peptide has also been shown to stimulate Na^+K^+ -ATPase and endothelial nitric oxide synthase activities.⁵ These results have led Wahren, et al.⁵ to propose the mechanism of action of C-peptide shown in Figure 2.4 below.

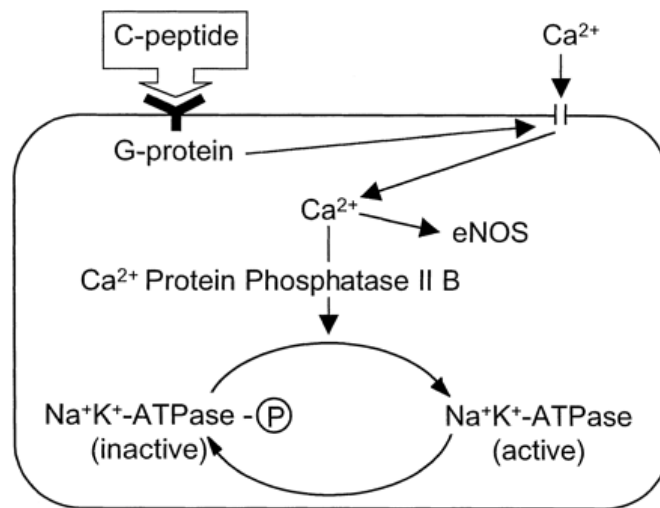


Figure 2.4. Proposed mechanism for C-peptide signaling cascade.⁵

Some studies have been conducted on the influence of C-Peptide on Atherosclerosis. Atherosclerosis is a common occurrence in diabetic patients. It is defined as the buildup of plaque in arteries that causes blockage and several cardiovascular disorders. C-Peptide has been

shown to induce an increase in Nitric Oxide in aortic cells to act as a pro-atherogenic effect.⁸ Interestingly, the dilation could not be replicated in other tissues. In endothelial cells, on the other hand, C-Peptide was shown to induce arteriolar dilation via nitric oxide dependent mechanisms. An overabundance of C-Peptide would cause inflammation, but a healthy amount causes dilation. (Figure 2.5)

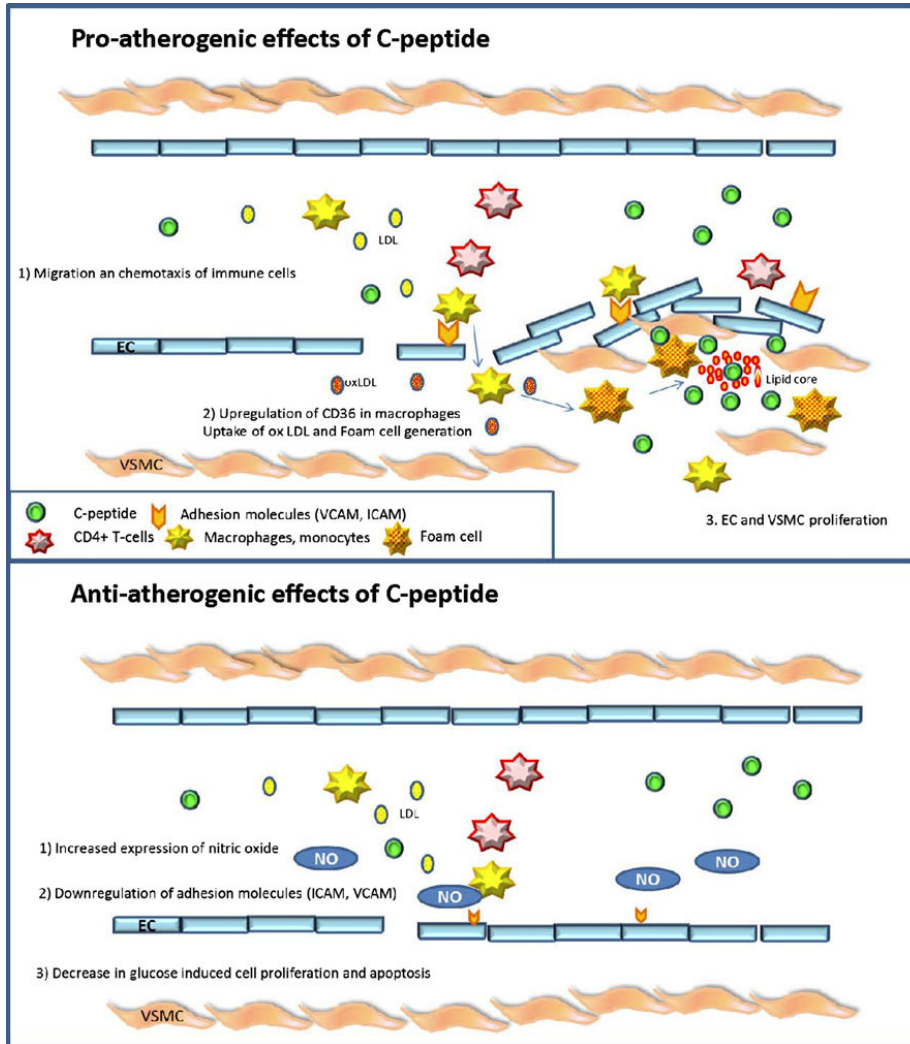


Figure 2.5. Depiction of the role of C-peptide in atherosclerosis.⁸

There have been several human studies conducted on people suffering from Type-1 diabetes. Low C-peptide levels in Type-1 patients is negatively correlated with microvascular

complications including retinopathy, neuropathy and nephropathy when compared to Type-2 patients.⁹ C-Peptide infusion in these patients leads to a nitric oxide mediated increase in arm blood flow while greatly reducing microalbuminuria and glomerular filtration rates.^{10,11} C-Peptide also helps to improve nerve conduction velocity and lessen autonomic dysfunction.¹²

Type-2 diabetics in early stages typically have considerably more C-Peptide than a non-diabetic and many negative complications of the disease can be correlated with the high C-Peptide levels. There is a positive correlation of fasting C-Peptide levels with cardiovascular death and mortality.¹³ Increased C-Peptide serum levels correlate with several risk factors for coronary artery disease including systolic blood pressure and dyslipidemia. There is a positive association with macrovascular complications in Diabetes Type-2 patients and C-Peptide levels.¹⁴ C-Peptide levels have a significant correlation with all-cause and cardiovascular deaths.¹⁵ Endothelial dysfunction and atherosclerosis can be found in Type-2 patients with high C-peptide levels.¹⁶

C-peptide was found to disrupt insulin aggregation in vitro as well as influence insulin to insulin interactions.¹⁷ These findings could be an explanation for why C-peptide is stored with insulin in the pancreas.

Lindahl et al. conducted an experiment similar to ours in premise.¹⁸ Biotinylated C-Peptide immobilized to an SA-chip has lysate run over it at 10 μ L/minute using 0.4% deoxycholate as the lysis detergent and employing human embryonic kidney (HEK-293) cell cultures as the tissue type. Any proteins found to bind with the C-Peptide were digested with trypsin, and analyzed with a MALDI-MS. A Peptide Mass Fingerprint was used to identify the proteins that could bind. They identified calcium-dependent serine protein kinase (CASK), as well as some cytoskeletal and cytoskeletal-associated proteins. CASK is a peripheral plasma

membrane protein, and a multi-domain scaffolding protein. It has a role in transmembrane protein anchoring and Ion channel control. Unlike most kinases, CASK does not require a divalent cation cofactor to operate catalytically. It binds to many cell-surface proteins found in the membrane. The authors believed most of their findings to be considered “sticky” proteins and did not offer a suggestion as to the reasoning for the binding capabilities to C-Peptide. We would like to improve upon their experiment in a couple of ways. Biotinylation takes advantage of the natural affinity of biotin for avidin. Avidin is a 66 kDa protein, and interactions between it and C-Peptide could easily be occurring. We proposed to use a different kind of affinity column that does not rely on protein interactions. Their detergent choice, deoxycholate, is typically considered a membrane detergent. Some of the cytosol proteins could have been lost and/or unfolded in the process. We proposed to use the more gentle NP-40 detergent. Their use of transformed HEK-293 cells is not optimal either because they are experimentally transformed and not a good model for the normal cell. For our experiment, we utilized animal tissue lysates.

This experiment was designed to identify cellular proteins capable of binding to C-peptide. A C-peptide affinity column was developed by attaching C-peptide to NHS magnetic beads by the N-terminus. Mouse heart, kidney and liver tissue samples were lysed and incubated with the affinity beads, before mass spectrometry was utilized to identify all the proteins capable of binding to these affinity magnetic beads. By identifying binding-partners, a better understanding can be gained about the cellular processes involving C-Peptide and could help to unlock the answers as to why the peptide is not degraded after its purpose of folding is complete. Upon the understanding of its purpose in the body, novel treatments could be developed to help diabetes patients, especially those suffering from Type-1.

Experimental Methods:

Preparation of C-Peptide Affinity Beads:

C-Peptide affinity beads were produced by covalently binding C-peptide to NHS PureProteome magnetic beads (Millipore) via primary amines (N-terminus and lysine residues) following the manufacturer's protocol. Briefly, 200 µg of human C-peptide was dissolved into 60 µL of phosphate buffered saline (PBS). To this solution, 30 µL of dimethylformamide (DMF) was added. Sixty µL of the 20% bead slurry was removed and added to a separate 1.5 mL microcentrifuge tube. This tube was placed into the magnetic stand, and the beads were allowed to migrate to the magnet facilitating removal of the buffer solution. Immediately, 500 µL of ice-cold equilibration solution (50/50 solution of distilled water and 1 M HCl) was added to the beads. The beads were then vortexed rigorously and placed back into the stand, and the solution was removed. Next, the C-peptide solution was added to the beads and the tube was removed from the stand. The beads were then incubated with continuous mixing at room temperature for 4 h. Afterwards, the beads were placed in the magnetic stand and allowed to migrate to the magnet before the unbound C-peptide solution was removed. The C-peptide solution removed was used to analyze bead binding efficiency. The magnetic beads attached to C-peptide were then vortexed rigorously for 30 s in 500 µL of Quench Buffer (100 mM Tris-HCl, 150 mM NaCl, pH 8.0). After mixing, the beads were placed back into the stand, and the solution was removed. This process was repeated another four times. A final 500 µL of the Quench Buffer was added and allowed to incubate with the beads at room temperature with continuous mixing for 1 h. The Quench Buffer was removed, and the beads were stored in 100 µL of PBS. The same procedure was followed for the creation of the pre-clear beads either with no peptide attached (skipping the incubation with C-peptide step) or substituting the C-peptide with the bradykinin peptide.

Tissue Lysis:

For these experiments, we isolated proteins from three types of mouse tissues, specifically: heart, kidney and liver. Mouse tissue was lysed using a NP 40 lysis buffer (50 mM Tris-HCl, 150 mM NaCl, 1% NP 40, pH 8.0) and manual grinding with mini grinders (Bio-Rad Ready Prep Mini Grinders). Protease inhibitors were added to the lysis buffer. Briefly, the tissue was homogenized in lysis buffer and allowed to sit on ice for 30 min to ensure optimal lysis of the tissue. The tissue lysate was then centrifuged at 12,000 G for 30 min at 4°C, and the supernatant lysate was transferred to a clean microcentrifuge tube. Pre-clear beads were added to the lysate to remove any proteins that had an affinity for beads themselves prior to incubation of the lysate with C-peptide beads.

Protein Isolation:

Proteins capable of binding to C-peptide were isolated using the affinity beads created above. We optimized all experimental conditions (time, temperature, etc.) until we were able to isolate proteins from different tissue lysates. Briefly, pre-cleared tissue lysates were incubated with C-peptide affinity beads for 4 h at room temperature or overnight at 4°C. After the reaction was complete, the beads were allowed to migrate to a magnet, the supernatant was removed, and the beads were washed once with phosphate buffered saline containing tween detergent (PBST) and twice with phosphate buffered saline (PBS). Then, 25 µL of SDS-Page loading buffer containing DTT was added to the beads, and the solution was heated for 5 min at 95°C to elute any captured proteins from the beads. The solution containing the eluted proteins was removed and placed into a clean microcentrifuge tube. The C-peptide beads were washed with PBST and PBS and stored in PBS at 4°C between uses.

SDS PAGE Analysis of Isolated Proteins:

Proteins isolated from the affinity columns were separated by sodium dodecyl sulfate-polyacrylamide gel electrophoresis (SDS-PAGE) prior to mass spectrometric analysis. Proteins were eluted from the affinity beads with the addition of SDS-PAGE sample loading buffer and loaded directly onto the PAGE TGX™ gels (4-15% gels, BioRad). Briefly, proteins were separated for 30 min at 200V using Tris/Glycine/SDS running buffer. DTT (0.1 M) was added directly to the samples, and all samples were heated for 5 min at 100°C prior to gel loading. Proteins were visualized with Bio-Safe Coomassie Stain (Bio-Rad).

Preparation of Tryptic Digests of Protein Samples from SDS-PAGE Bands:

Protein bands from the SDS-PAGE gels were excised, reduced with DTT, treated with iodoacetamide, and digested with trypsin overnight at room temperature following the procedure at <http://ms-facility.ucsf.edu/ingel.html>.

Briefly, protein bands were excised from gel, diced into smaller pieces and placed in 0.5 mL siliconized microcentrifuge tubes. 100 µL of 25 mM NH₄HCO₃/50% ACN was added to the gel pieces and vortexed for 10 min. A gel loading tip was used to extract the supernatant that was discarded. This was repeated twice more until the gel pieces no longer contained visible staining. Next, a fresh solution of 10 mM DTT in 25 mM NH₄HCO₃ was prepared. About 25 µL of DTT was added to each tube. They were vortexed and spun briefly before being allowed to incubate at 56° C for 1 h. The supernatant was then removed and discarded, and 30 µL of a freshly prepared 55 mM iodoacetamide in 25 mM NH₄HCO₃ was added to the gel pieces. These were allowed to incubate in the dark for 45 min. The supernatant was then removed, and 100 µL of NH₄ HCO₃ was added to wash the gels and was then removed. Next, the gels were washed twice with 100 µL of 25 mM NH₄HCO₃/50% ACN. All supernatants were removed. Then, a solution containing

0.2 µg trypsin in 30 µL of 25 mM NH₄HCO₃ was added to each gel piece and allowed to digest overnight at room temperature. The digest solution was transferred into a clean tube, and to the gel pieces, 30 µL of 50% ACN/5% formic acid was added, and vortexed for 30 min. These were then spun down and sonicated. The solution was removed and added to the digest solution in the clean tube. The process was then repeated once more. The resulting digest solution was then lyophilized (Savant SpeedVac) to a volume of about 10 µL.

Analysis of Tryptic Digests of Proteins by MALDI-TOF Mass Spectrometry:

The tryptic digests of the proteins were purified with C₁₈ ZipTips (Millipore) and analyzed on a Bruker Autoflex MALDI-TOF mass spectrometer (Billerica, MA). Prior to analysis, the peptide preparations (0.6 µL) were each mixed with a 50% aqueous acetonitrile solution (0.6 µl) of saturated α-cyano-4-hydroxy-cinnamic acid containing 0.05% TFA as matrix, spotted onto a stainless steel sample plate and allowed to air dry. The mass spectra were recorded in positive ion mode with a 60 nsec delay in the m/z range from 500 to 3500. Typically, ~1000 spectra were accumulated with 50 laser shots for each sample spot analyzed. The resulting peptide mass fingerprint spectra obtained for each protein analyzed was used to identify the protein by inputting the peptide molecular weights obtained into the mascot search engine (Matrix Science Ltd. (2008) MASCOT peptide mass fingerprint.

http://www.matrixscience.com/cgi/search_form.pl?FORMVER=2&SEARCH=PMF).

Analysis of Tryptic Digests of Proteins by LC/ESI/MS:

The tryptic digest of the proteins were fractionated on 10µm spherical C₁₈ resins (YMC, Inc. Milford, MA) and were eluted directly into the electrospray source of a ThermoFinnigan LCQ mass spectrometer (ThermoScientific, Waltham, MA) equipped with a quadrupole ion trap mass analyzer. The reverse phase microcapillary columns were constructed according to a

procedure modified from Kennedy and Jorgensen.¹⁹ The loading of peptides onto the columns was performed using a helium bomb. Once applied to the columns, the peptides were first washed with 0.1% acetic acid for 3 min and were then collectively eluted from the columns with 60% acetonitrile in 0.1% acetic acid at a flow rate of 2 $\mu\text{L}/\text{min}$ using the helium bomb. The column elutes directed into the electrospray source were analyzed by MS and tandem mass spectrometry (CID fragmentation with He) favoring isolation and fragmentation of doubly charged ions.

The ESI/MS system was operated with the Xcalibur software (version 2.0, ThermoFinnigan), with the same software used also for data analysis. The mass spectrometer was set to function in the positive ion mode with parameters optimized during direct infusion of peptide standards with solvent. The solvent, consisting of 50/50 (v/v) 0.1% acetic acid in water/acetonitrile, was applied at a flow rate of 3 $\mu\text{L}/\text{min}$. Nitrogen was used as the sheath gas (setting at 60), and ultrapure helium was used as the collision gas. The ion spray voltage was set as 4.5 kV and the capillary temperature was 210°C.

Results and Discussion:

C-peptide, once thought to be an inactive peptide merely existing to help in the folding of insulin, could actually have a more active role in the body. Little is known of the active function of this peptide in the body, but evidence suggests it has a reason to remain in the body because it is not degraded immediately after the formation of mature insulin is complete. In fact, C-peptide has a longer half-life in the body than insulin. Previous studies have attempted to identify molecules and proteins that can bind to C-peptide, but they have not found substantial results.

This experiment was designed to gain an improved understanding of the cellular actions of C-peptide by examining what proteins a C-peptide affinity column would extract from three different mouse tissue lysates of heart, kidney and liver. Kidney tissue was chosen because the clinical data obtained from C-peptide replacement therapy showed that C-peptide ameliorated diabetic nephropathy indicating that C-peptide may protect the kidneys from damage caused by hyperglycemia. The kidney was our main tissue of interest, but we also decided to study heart tissue because C-peptide is correlated with cardiovascular disorders. We also chose to study liver tissue because the liver is the main target organ of mature insulin.

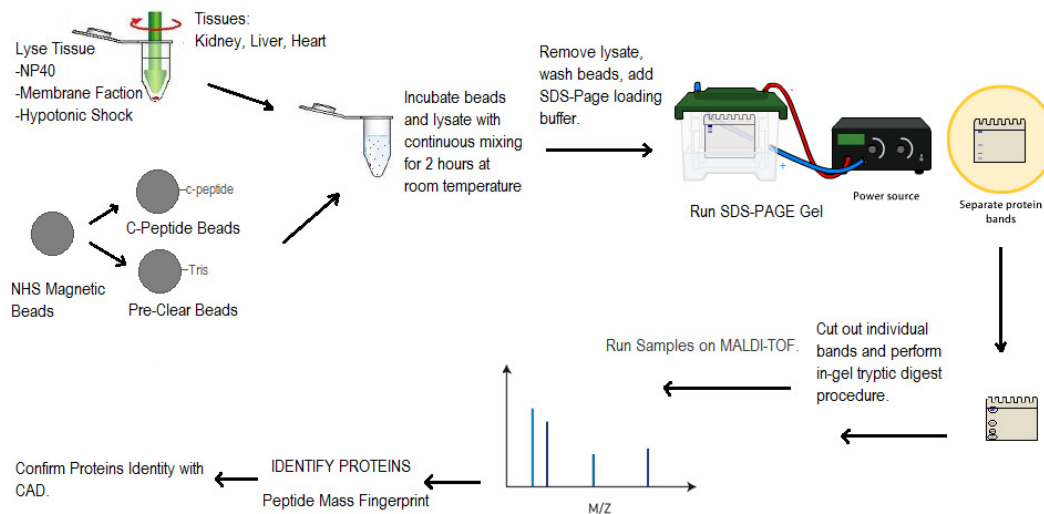


Figure 2.6. Basic experimental protocol for protein isolation using the C-peptide affinity beads.

The basic protocol for this experiment is summarized in Figure 2.6. We developed C-peptide affinity beads by attaching C-Peptide via its N-terminus to the NHS magnetic beads. We then lysed heart, kidney and liver mouse tissues and incubated pre-cleared cellular lysates with the affinity beads for 3 h at room temperature. Proteins isolated from the affinity beads were

separated by reducing SDS-PAGE, digested with trypsin, and analyzed via MALDI-TOF mass spectrometry.

The proteins bands excised from the SDS-PAGE gels were identified by mass spectrometry through the Peptide Mass Fingerprint (PMF) technique. In PMF, an unknown protein is cleaved into smaller peptide fragments using a specific protease, most commonly trypsin. The molecular weight of each fragment peptide is then accurately measured by mass spectrometry. These peptide masses are then compared to a computer database of known protein sequences. Mascot, a computer program, works to take the unknown sequence from the database and compares them with the masses in order to determine a protein match. In this experiment, the proteins isolated were identified via excising a protein band from the gel, digesting the protein with trypsin, and analyzing the resulting peptide fragments with MALDI-TOF mass spectrometry.

Results from Trial 1 Using Tris Pre-clear Beads:

The experiment described above was conducted using Tris pre-clear beads and C-peptide beads to isolate proteins from both mouse kidney and liver tissue. The SDS-PAGE gel of the isolated proteins can be seen in Figure 2.7. Lane E contained the molecular weight standard while A and B contained mouse kidney pre-clear and C-peptide, respectively, and lanes C and D contained mouse liver pre-clear and C-peptide, respectively.

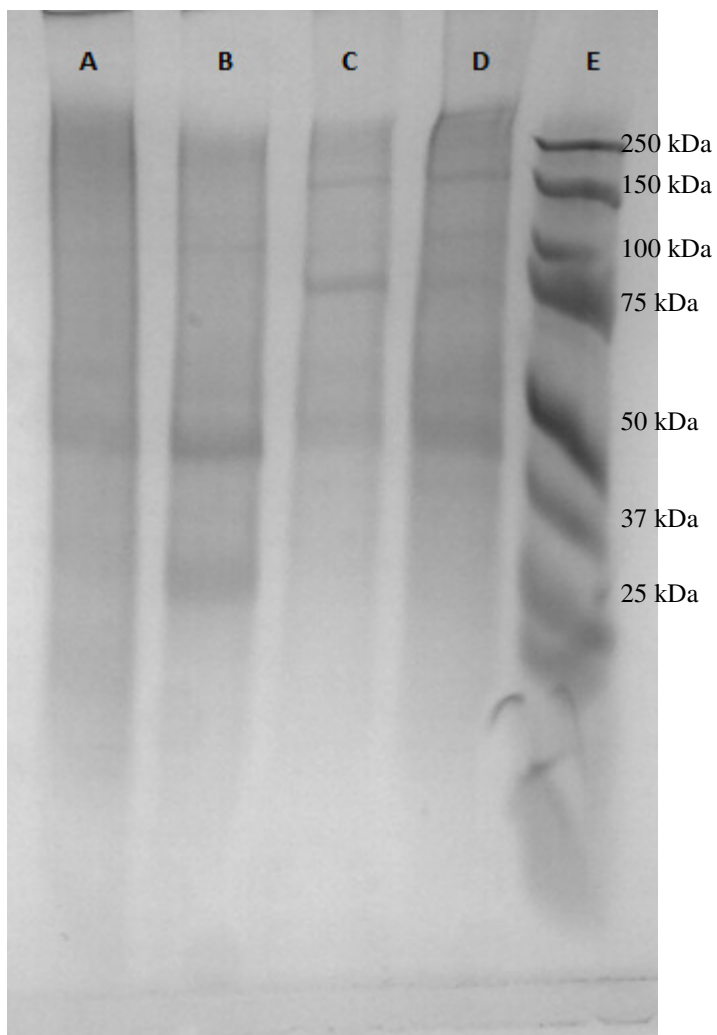


Figure 2.7. SDS-PAGE Gel separation of proteins. Lanes: A. Mouse Kidney Lysate pre-clear, B. Mouse Kidney Lysate C-peptide, C. Mouse Liver Lysate pre-clear, D. Mouse Liver Lysate C-peptide and E. molecular weight standards.

Proteins Isolated from Kidney Tissue by C-peptide Beads:

The MALDI-TOF mass spectrum generated from the tryptic digest of the protein at about 25 kDa in lane B of the SDS PAGE gel (in figure 2.7) is shown in Figure 2.8. The protein band had no counterpart protein present in the pre-clear control lane. This protein was identified as the dihydrolipoyllysine-residue acetyl transferase component (E2) of pyruvate dehydrogenase.

The same area was excised from the pre-clear lane, and no peptide fragments were observed as expected that indicated that this protein was specifically isolated by the C-peptide beads only. This protein has a molecular weight of 67.9 kDa that does not match up with the approximate 25 kDa position in the gel. This discrepancy needed to be investigated further. When the observed tryptic peptides are examined, they all originate from the C-terminal portion of the protein as shown in Figure 2.9. This suggests that we are isolating a truncated form of this protein that originates from either a proteolytic cleavage or through alternate splicing of the protein (isoform). Pyruvate dehydrogenase is actually an enzyme complex that catalyzes the overall conversion of pyruvate to acetyl-CoA and CO₂. The complex contains multiple copies of three enzymatic components: pyruvate dehydrogenase (E1), dihydrolipoamide acetyltransferase (E2) and lipoamide dehydrogenase (E3). When activity of the E2 protein is examined, it reveals that the N-terminus portion contains the E1 and E3 component binding domains for attachment of E2 to the pyruvate dehydrogenase complex. The C-terminal portion of E2 contains the enzymatic activity of the protein. E2 utilizes a transacetylation reaction that transfers an acetyl group to the thiol in Coenzyme A thus forming acetyl-CoA. The reaction schematic can be seen in Figure 2.10. Perhaps a truncated version of this protein would produce an enzyme independent of the pyruvate dehydrogenase complex that would be able to perform transacetylations on other molecules. We could find no previous research about known alternative splicing variants of this protein.

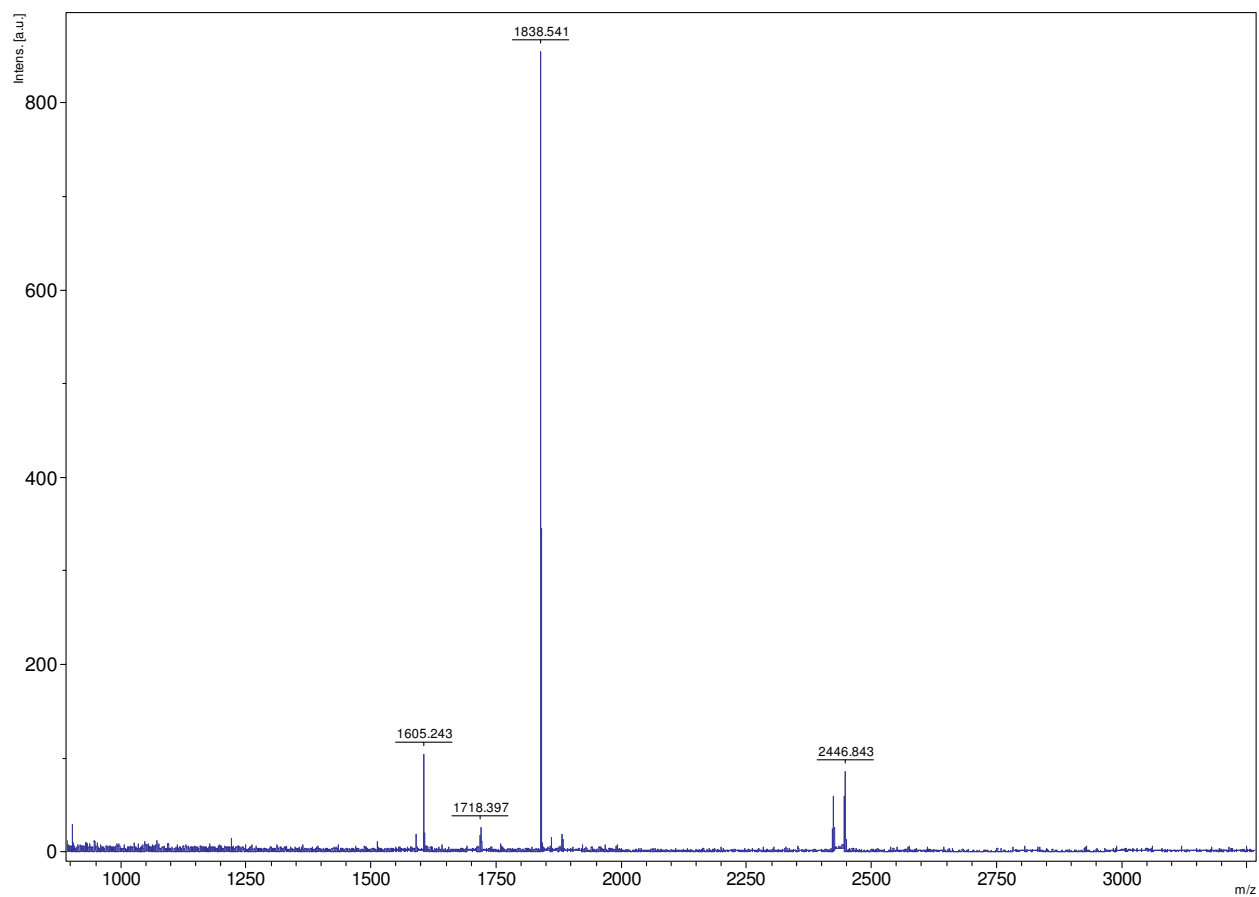


Figure 2.8. MALDI-TOF peptide fingerprint mass spectrum for the protein excised from the band at 25 kDa in the C-peptide lane of the SDS-PAGE gel for mouse kidney in Lane B of Figure 2.7.

Matched peptides shown in **bold red**.

```

1 MWRVCARRAR SAVPRDGFRA RWAALKEGPG APCGSPRIGP AAVRCGSGIP
51 RYGVRSLCGW SSGSGTVPRN RLLRQLLGSP SRRSYSLPPH QKVPLPSLSP
101 TMQAGTIARW EKKEGEKISE GDLIAEVETD KATVGFESLE ECYMAKILVP
151 EGTRDVPVGS IICITVEKPQ DIEAFKNYTL DLAAAAAPQA APAAAPAPAA
201 APAAPSASAP GSSYPHMQI VLPALSPTMT MGTVQRWEKK VGEKLSEGD
251 LAEIETDKAT IGFEVQEEGY LAKILVPEGT RDVPLGAPLC IIVEKQEDIA
301 AFADYRPTFV TSLKPQAAPP APPFVAAVPP TPQPVAPTPS AAPAGPKGRV
351 FVSPLAKKLA AEKGIDLTQV KGTGPEGRII KKDIDSFVPS KAAPAAAAAM
401 APPGPRVAPA PAGVFTDIPI SNIRRVIAQR LMQSKQTIPH YYLSVDVNMG
451 EVLLVRKELN KMLEGKGIS VNFIIKASA LACLKVPEAN SSWMDTVIRQ
501 NHVVDVSVAV STPAGLITPI VFNAHIKGLE TIASDVVSLA SKAREGKLQP
551 HEFQGGTFTI SNLGMFGIKN FSAIINPPQA CILAIGASED KLIPADNEKG
601 FDVASVMSVT LSCDHRVVDG AVGAQWLAEF KKYLEKPITM LL

```

Figure 2.9. The amino acid sequence of the dihydrolipoyllysine-residue acetyl transferase component (E2) of pyruvate dehydrogenase protein. The peptide sequences observed in the mass fingerprint spectrum (Figure 2.8) are shown in red.

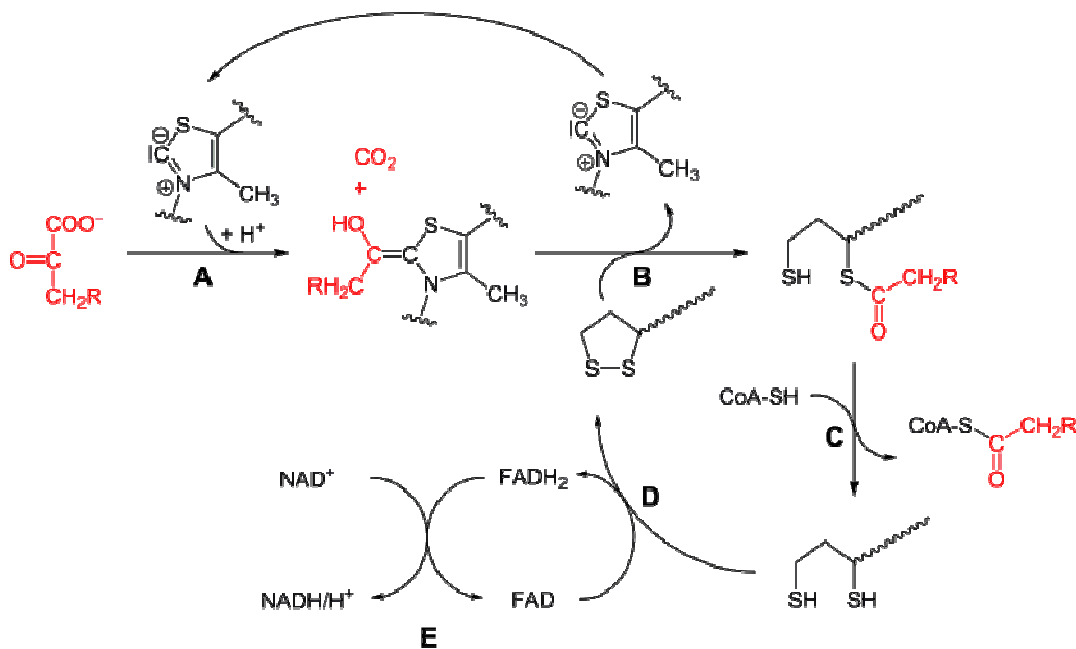


Figure 2.10. Schematic of oxidation decarboxylation of pyruvate as catalyzed by the pyruvate dehydrogenase complex. Reaction C is catalyzed by the dihydrolipoyllysine-residue acetyl transferase component (E2).

The band excised from the 40 kDa position in lane B of the SDS-PAGE gel for mouse kidney C-peptide (Lane B in Figure 2.7) was identified as long-chain specific acyl-CoA dehydrogenase (ACADL). The MALDI-TOF mass spectrum generated from the tryptic digest of this protein is shown in Figure 2.11. ACADL is an oxidoreductase enzyme that catalyzes the reaction of the reduction of an acceptor using acyl-CoA to 2,3-dehydroacyl-CoA (reaction is shown in Figure 2.12). Its primary purpose is in mitochondrial fatty-acid beta-oxidation and lipid metabolism.

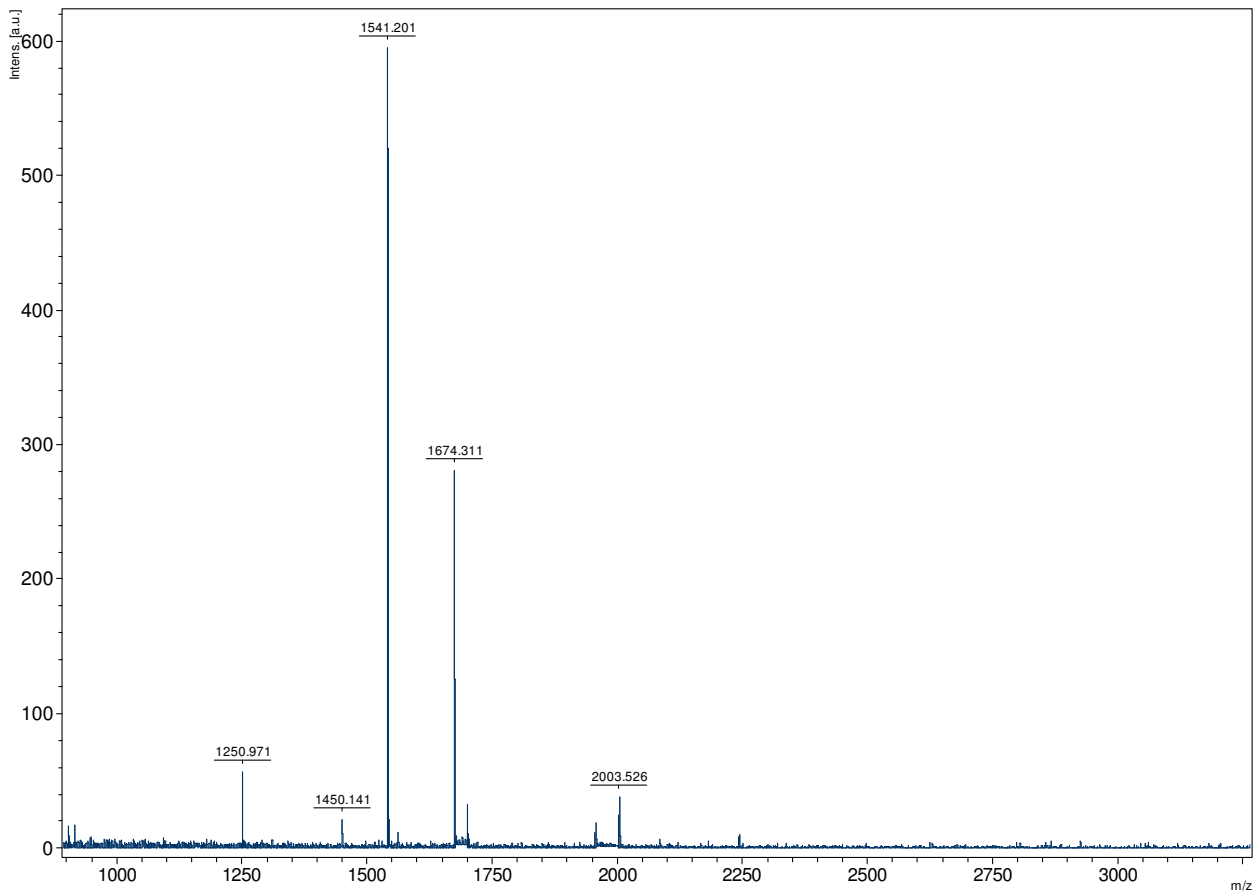


Figure 2.11. MALDI-TOF peptide fingerprint mass spectrum for the protein excised from the protein band at 50 kDa in the C-peptide lane of the SDS-PAGE gel for mouse kidney in Lane B of Figure 2.7.

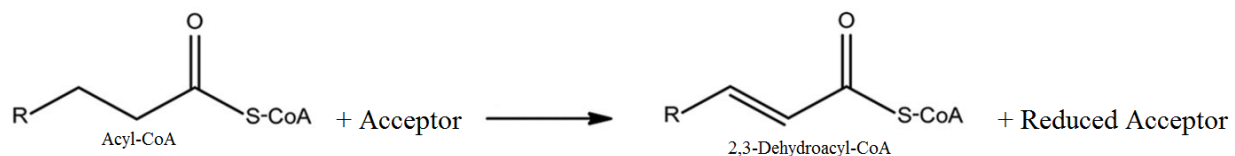


Figure 2.12. Basic reaction catalyzed by long-chain specific acyl-CoA dehydrogenase.

Proteins Isolated from Liver Tissue by C-peptide Beads:

The MADLI-TOF mass spectrum generated from the tryptic digest of the protein excised from the band at 50 kDa in the C-peptide experimental lane D for mouse liver (Figure 2.7) is shown in Figure 2.13. The peptide mass fingerprint search using Mascot identified this protein as aldehyde dehydrogenase 2, ALDH2. This protein was not found in the control pre-clear lane, indicating that it was a unique protein that was only isolated with the C-peptide beads. The ALDH2 enzyme, localized inside the mitochondrial matrix, can oxidize reactive aldehydes into non-reactive carboxylic acids. Because aldehydes are highly reactive molecules in the body they act as intermediates or products involved in a wide area of biologic, physiologic and pharmacologic processes. In general, aldehydes are created during the metabolism and synthesis of amino acids, lipids, carbohydrates and drugs and during the biosynthesis of retinoic acid. ALDH2 plays a critical role in the process of detoxification of the products of lipid peroxidation, even though it is typically known for its role in the metabolism of alcohols. Evidence suggests ALDH2 can protect against both microvasculature and microvasculature against reactive aldehydes created in situations of oxidative stress on a system,²⁰ that can be connected to neuropathy and retinopathy associated with diabetes. There are also several human diseases that ALDH2 dysfunction may have a role in causing including cardiovascular disease, diabetes, neurodegenerative diseases, stroke and cancer.²¹ It has been shown that ALDH2 expression is

dramatically decreased with the progression of diabetes, while the activation of ALDH2 with ethanol can decrease diabetes induced myocardial injury.²² C-peptide binding to ALDH2 may result in an effect in its activity. Alternatively, it could be entering the nucleus in cells and affecting the expression levels of ALDH2, so future work could be to determine the mRNA levels of ALDH2 produced when cultured cells are exposed to C-Peptide, that could lead to a decrease in activation of ALDH2 and an increase in concentrations of damaging reactive oxygen species (ROS) within the cells. An increase in ROS production has been shown to be a mediator of hyperglycemic tissue injury.²³

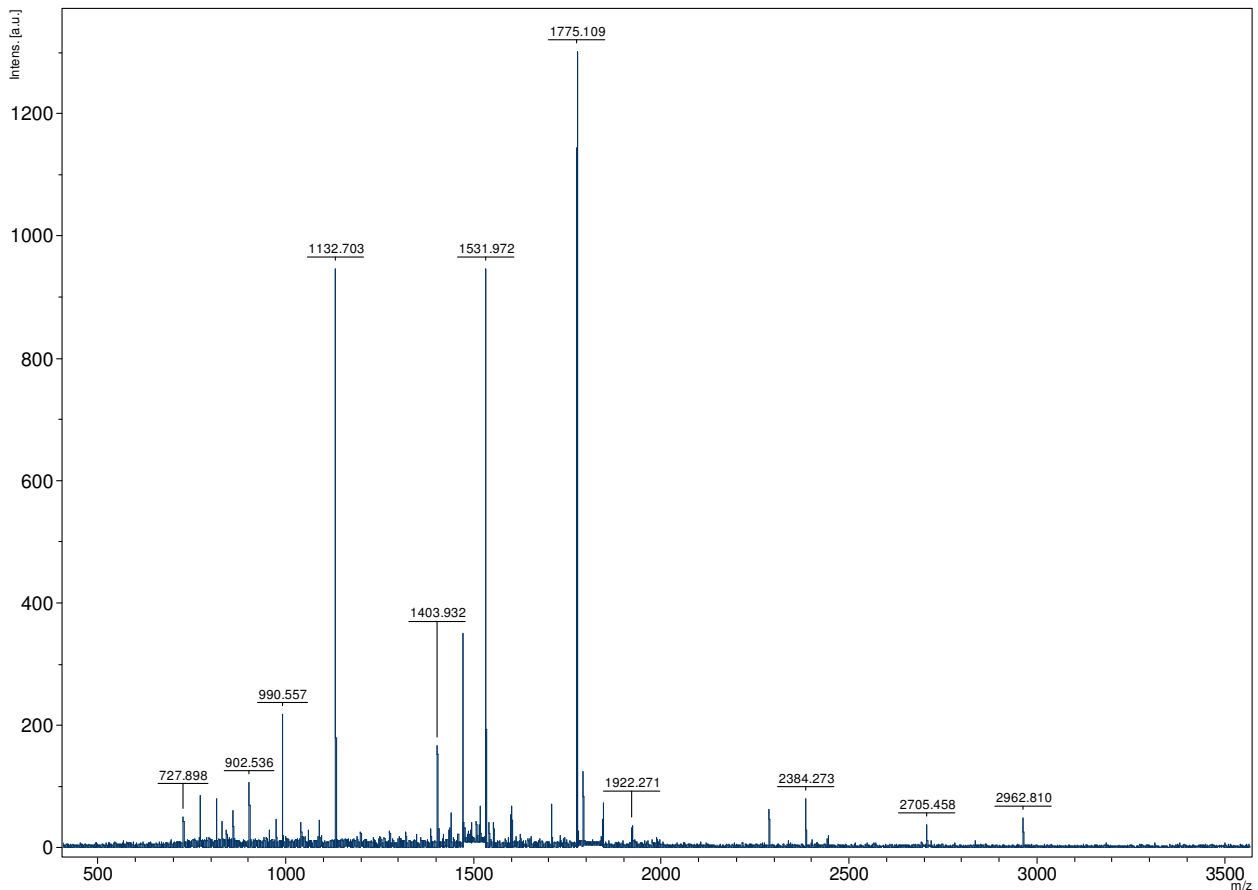


Figure 2.13. MALDI-TOF peptide fingerprint mass spectrum for the protein excised from the band at 50 kDa in the C-peptide lane of the SDS-PAGE gel for mouse liver in Lane D of Figure 2.7.

The MALDI-TOF mass spectrum shown in Figure 2.14 is the tryptic digest for the band excised at 100 kDa in the C-peptide experimental lane D for mouse liver of the SDS-PAGE gel (Figure 2.7). The protein was identified via peptide mass fingerprint database search using the Mascot search engine to be the major vault protein, MVP. This protein has no corresponding band in the pre-clear control lane, indicating it is unique to C-peptide binding. Very little information is known about the biological function of vaults. They are composed of mostly MVP subunits by mass, and have an evolutionarily conserved amino acid sequence. They are related to chemotherapy resistance, transport mechanisms in the cell, signal transduction, and immune response.²⁴ Because so little is known about this protein, conclusions involving its relationship with c-peptide would be purely speculation. It could be involved with cell transport of the peptide throughout the cytosol of cells, and it could assist with the movement of the C-peptide into the nucleus of cells.

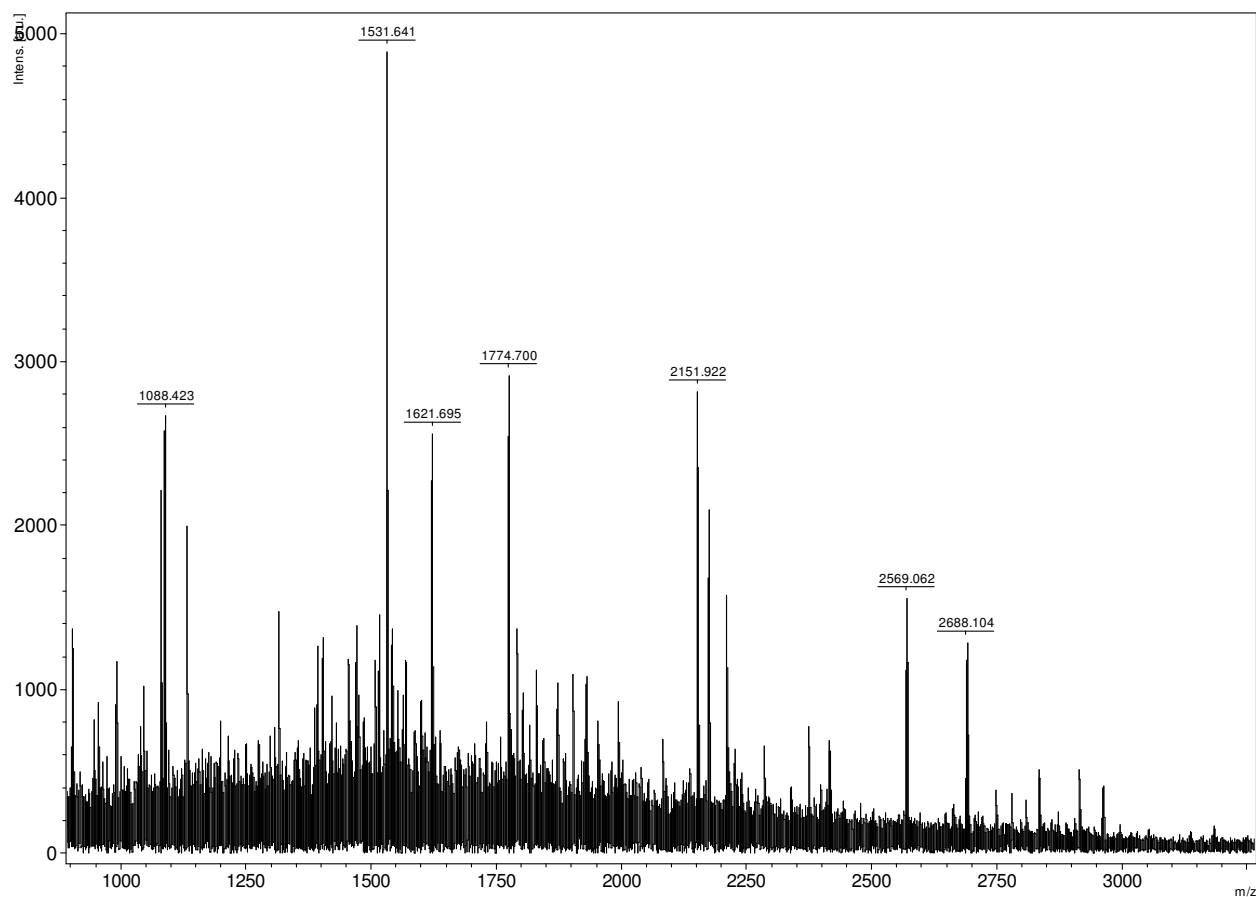


Figure 2.14. MALDI-TOF peptide fingerprint mass spectrum for the protein excised from the band at 100 kDa in the c-peptide liver lane (D) of the SDS-PAGE gel shown in Figure 2.7.

Results from Trial 2 using Bradykinin Pre-clear Beads:

The previous experiment was repeated, and the only change was the use of bradykinin pre-clear beads in place of the regular Tris pre-clear beads. This was done in hopes to rule out any interaction that is the result of non-specific binding between a peptide and a protein. Bradykinin (pictured in Figure 2.15) was a good choice for this substitution, at nine amino acids in length; it contains a pair of arginines that are typically positively charged at pH 7.4 and polar and hydrophobic amino acids. It does lack acidic residues that would have been helpful for ruling out any electrostatic interactions based upon binding to negative regions on our C-peptide. Ideally, we wanted to use a scrambled C-peptide sequence to create the pre-clear beads, but

funds were not available to purchase this peptide. Bradykinin is a bioactive peptide whose interactions are known to primarily affect blood vessels, and have no known interactions with any of the tissue types worked with during the course of this experiment. Again, mouse kidney, heart, and liver tissues were lysed, the lysates were pre-cleared with bradykinin beads, and the proteins were then isolated with the same C-peptide beads used in the first experiment. The isolated proteins were eluted from the beads, separated by SDS-PAGE electrophoresis, and visualized with Coomassie stain. The resultant SDS-PAGE gel is shown in Figure 2.16. Lane C of the gel contained molecular weight markers. Lanes A and B came from mouse kidney lysate, with A being the pre-clear bradykinin beads and B being the C-peptide beads. Lanes D and E came from the mouse heart lysate with D being the pre-clear bradykinin beads and E being the C-peptide. Lanes F and G came from the mouse liver lysate with F being the pre-clear bradykinin and G being the C-peptide beads. Several protein bands appeared in each lane, and a total of 16 of the protein bands were excised and further analyzed by mass spectrometry. There were no bands observed in the heart lysates that differed between the C-peptide and pre-clear lanes in the gel, so no proteins bands from the heart lysates were analyzed further.

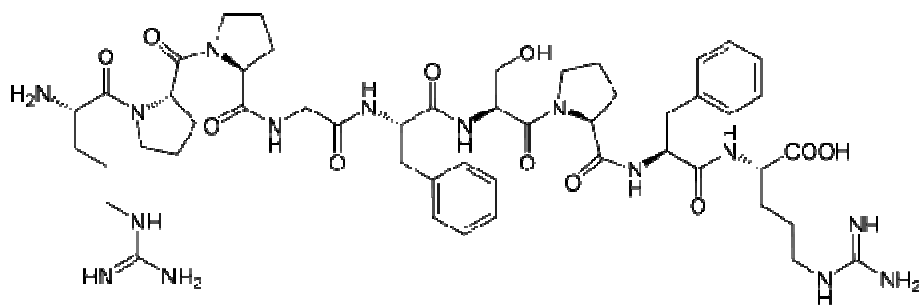


Figure 2.15. The amino acid structure of the peptide Bradykinin. Amino acid sequence: Arg-Pro-Pro-Gly-Phe-Ser-Pro-Phe-Arg

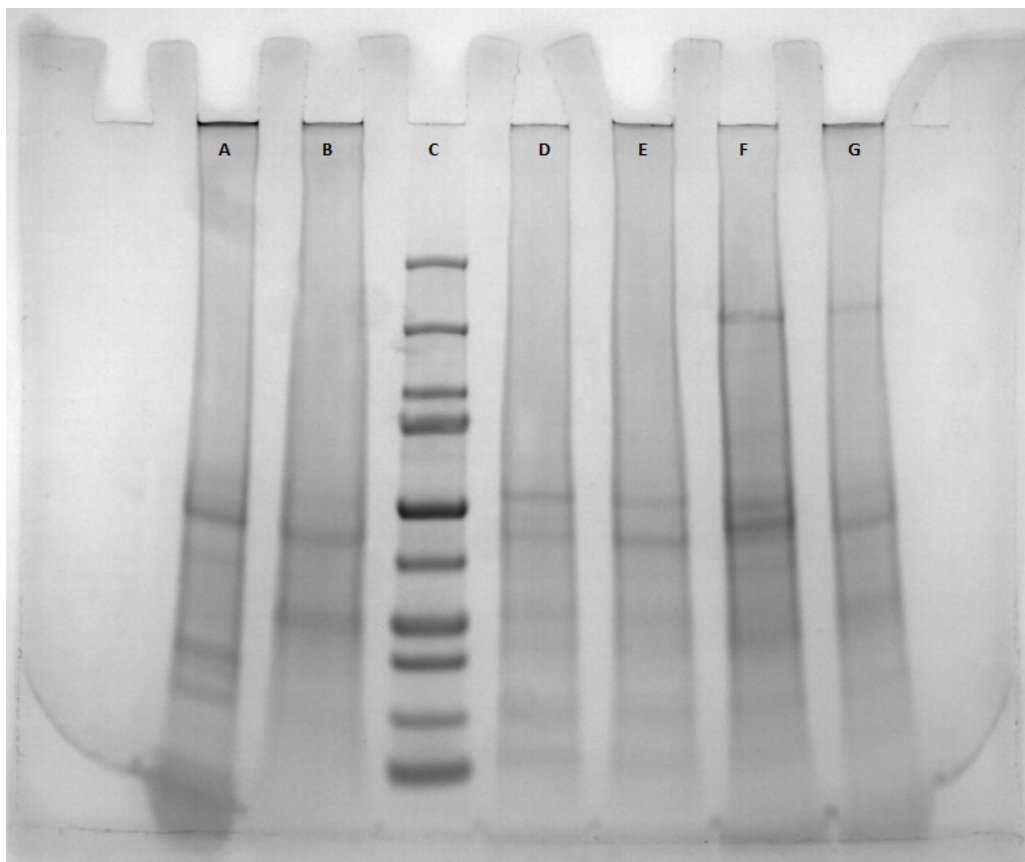


Figure 2.16. SDS-PAGE Gel separation of proteins, Lanes: A. Mouse Kidney Bradykinin Pre-clear, B. Mouse Kidney C-Peptide, C. Molecular weight standard, D. Mouse Heart Bradykinin Pre-Clear, E. Mouse Heart C-Peptide, F. Mouse Liver Bradykinin pre-clear, G. Mouse Liver C-Peptide. Protein bands were excised from the gel for further analysis.

Proteins Isolated from Liver Tissue by C-peptide Beads:

The protein bands at about 50 kDa liver lanes were excised and identified via peptide mass fingerprint. The protein from both lanes was identified as ALDH2. Figure 2.17 shows the mass spectra obtained from the tryptic peptides generated from the protein in the C-peptide lane and bradykinin lane. Several of the peptide peaks match up. Pulling out ALDH2 in the bradykinin control lane as well as the C-peptide lane suggests that it is a simple matter of peptide interactions that ALDH2 would bind to C-peptide. The quality of the spectra is increased in the

pre-clear bradykinin lane which makes sense considering the procedure in that the bradykinin beads get a chance to bind in the lysate first. It is for this reason that we believe C-peptide's interactions with ALDH2 is the result of nonspecific peptide binding.

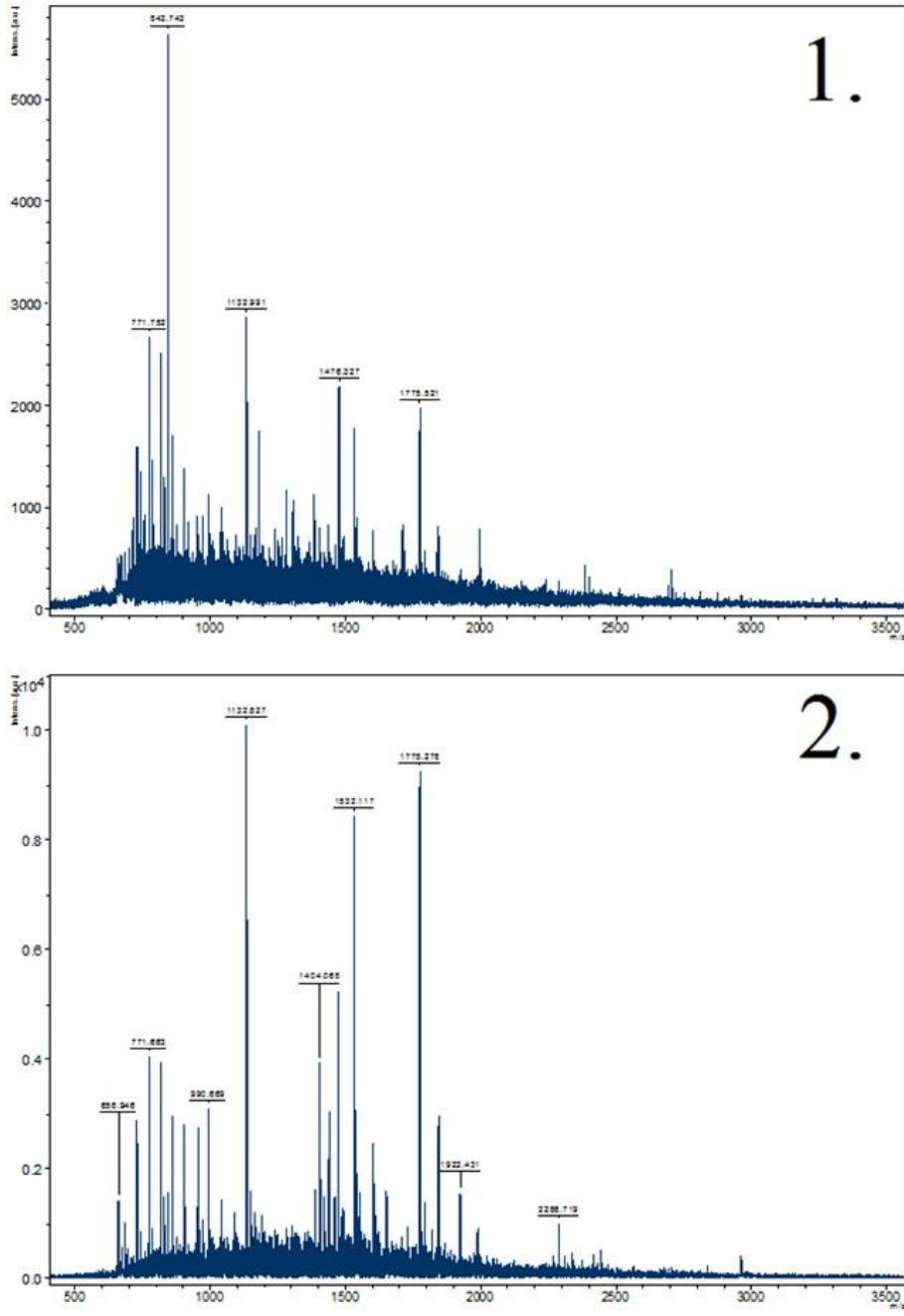


Figure 2.17. MALDI-TOF peptide fingerprint mass spectra for the protein excised from the band at 50 kDa in the C-peptide (1.) and bradykinin (2.) lanes of the SDS-PAGE gel for mouse liver in Lane G and F, respectively, shown in Figure 2.16.

Proteins Isolated from Kidney Tissue by C-peptide Beads:

The MALDI-TOF mass spectrum shown in Figure 2.18 is the tryptic digest for the protein band excised at 40 kDa in the C-peptide experimental lane B for mouse kidney of the SDS-PAGE gel (Figure 2.16). The protein was identified via peptide mass fingerprint database search using the Mascot search engine to be long-chain specific acyl-CoA dehydrogenase (ACADL). The spectrum was not as good as that obtained in the first trial, but there were enough peptide peaks to successfully identify the protein. The fact that we were able to isolate this same protein from the kidney lysate with our C-peptide beads strengthens our findings that this protein is a cellular target of the C-peptide. Our only concern is that we would have expected to isolate this protein from other tissue lysates, so more work will need to be done to look into why we only seem to pull out this protein from the kidney lysates.

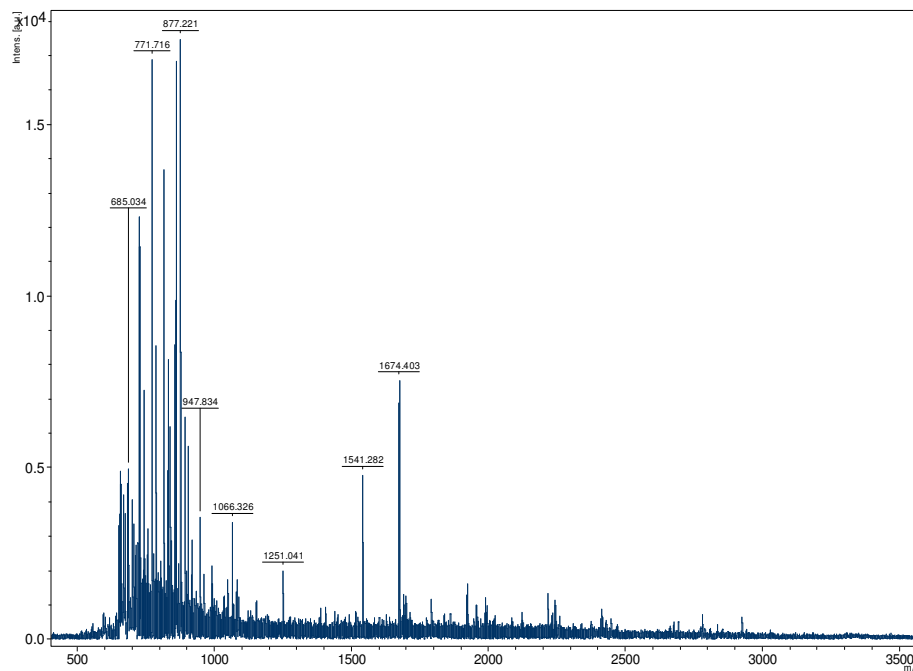


Figure 2.18. MALDI-TOF peptide fingerprint mass spectrum for the protein excised from the band at 40 kDa in the C-peptide lane of the SDS-PAGE gel for mouse kidney in Lane B (Figure 2.16).

The peptide mass fingerprint spectrum obtained for the protein band excised at 25 kDa in the C-peptide experimental lane B for mouse kidney of the SDS-PAGE gel (Figure 2.16) is shown in Figure 2.19. The protein was identified as dihydrolipoyllysine-residue acetyltransferase (E2) component of pyruvate dehydrogenase complex for a second time, with a higher mascot score of 87. The gel had no corresponding band in the bradykinin lane A (as seen in Figure 2.16), suggesting this is a specific binding for C-peptide. Once again when the peptides observed in the spectrum were matched up with the known amino acid sequence of this protein (Figure 2.20), the observed peptides were only from the C-terminal portion of the protein, suggesting an alternatively spliced protein or a cleaved protein. The repeat identification of this protein with no counterpart in the control lane suggests it is a good binding partner for C-peptide. Its appearance in the 25kDa position of the gel and the repeat incidence of the peptides matching to the C-terminus suggests a more purposeful reason for the smaller protein fragment. To confirm the identity of this protein, we sequenced the peptide at m/z 1839 by tandem mass spectrometry. The resulting CID MS/MS mass spectrum for the fragmentation of this peptide is shown in Figure 2.21. Analysis of the y and b fragment ions observed in the CID spectrum revealed that this peptide had a sequence consisting of VAPAPAGVFTDIPISNIR that corresponded to the correct peptide sequence for the E2 protein.

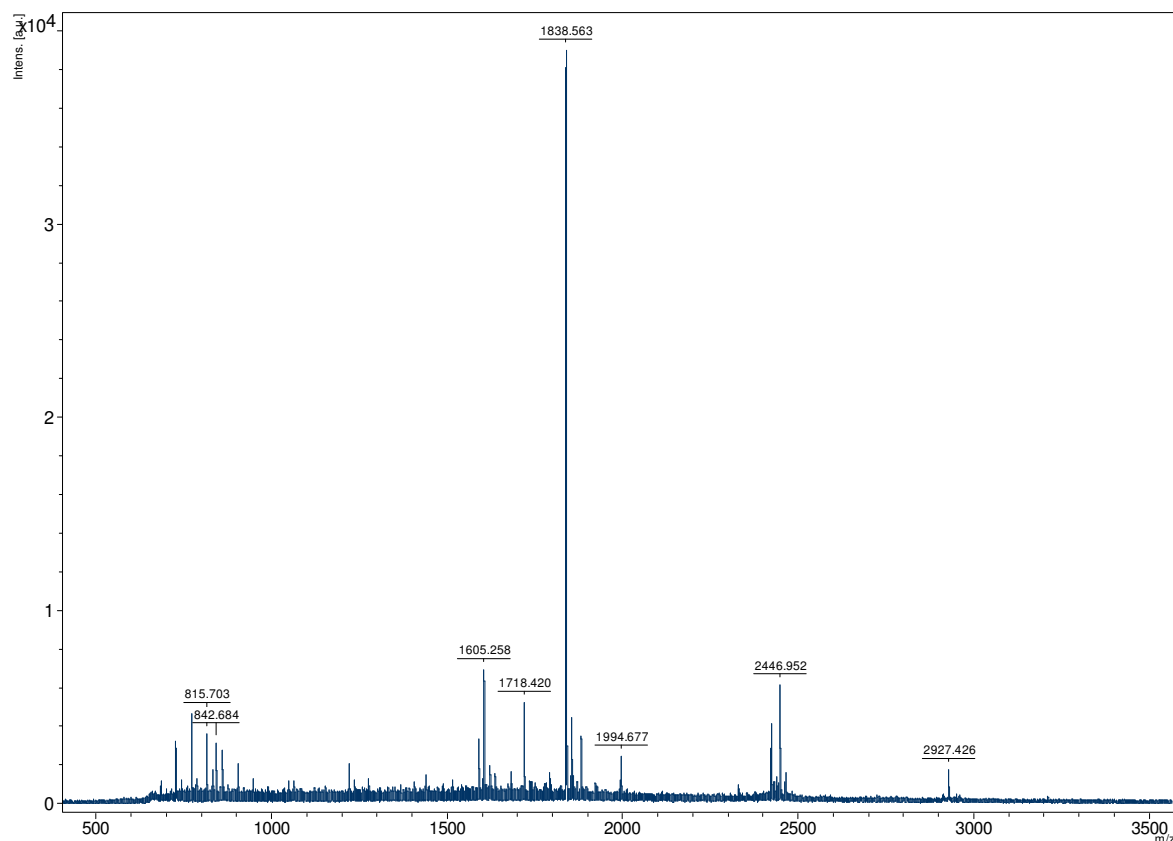


Figure 2.19. MALDI-TOF peptide fingerprint mass spectrum for the protein excised from the band at 25 kDa in the c-peptide lane of the SDS-PAGE gel for mouse kidney in Lane B.

Matched peptides shown in **bold red**.

```

1 MWRVCARRAR SAVPRDGFRA RWAALKEGPG APCGSPRIGP AAVRCGSGIP
51 RYGVRSLCGW SSGSGTVPRN RLLRQLLGSP SRRSYSLPPH QKVPLPSLSP
101 TMQAGTIARW EKKEGEKISE GDLIAEVETD KATVGFESLE ECYMAKILVP
151 EGTRDVPVGS IICITVEKPQ DIEAFKNYTL DLAAAAAPQA APAAAPAPAA
201 APAAPSASAP GSSYPHMQI VLPALSPTMT MGTVQRWEKK VGEKLSEGDL
251 LAEIETDKAT IGFEVQEEGY LAKILVPEGT RDVPLGAPLC IIVEKQEDIA
301 AFADYRPTEV TSLKPQAAPP APPPVAAVPP TPQPVAPTSP AAPAGPKGRV
351 FVSPLAKKLA AEKGIDLTQV KGTGPEGRII KKDIDSFVPS KAAPAAAAAM
401 APPGPRVAPA PAGVFTDIPI SNIRRVIAQR LMQSKQTIPH YYLSVDVNMG
451 EVLLRKELN KMLEGKGIS VNDFIIKASA LACLKVPEAN SSWMDTVIRQ
501 NHVVDVSAV STPAGLITPI VFNAHIKGLE TIASDVVSLA SKAREGKLQP
551 HEFQGGTFTI SNLGMFGIKN FSAIINPPQA CILAIGASED KLIPADNEKG
601 FDVASVMSVT LSCDHRVVDG AVGAQWLAEF KKYLEKPITM LL

```

Figure 2.20. The Matrix Mascot search results for the matched peptide sequences found for the peptide peaks observed in Figure 2.19.

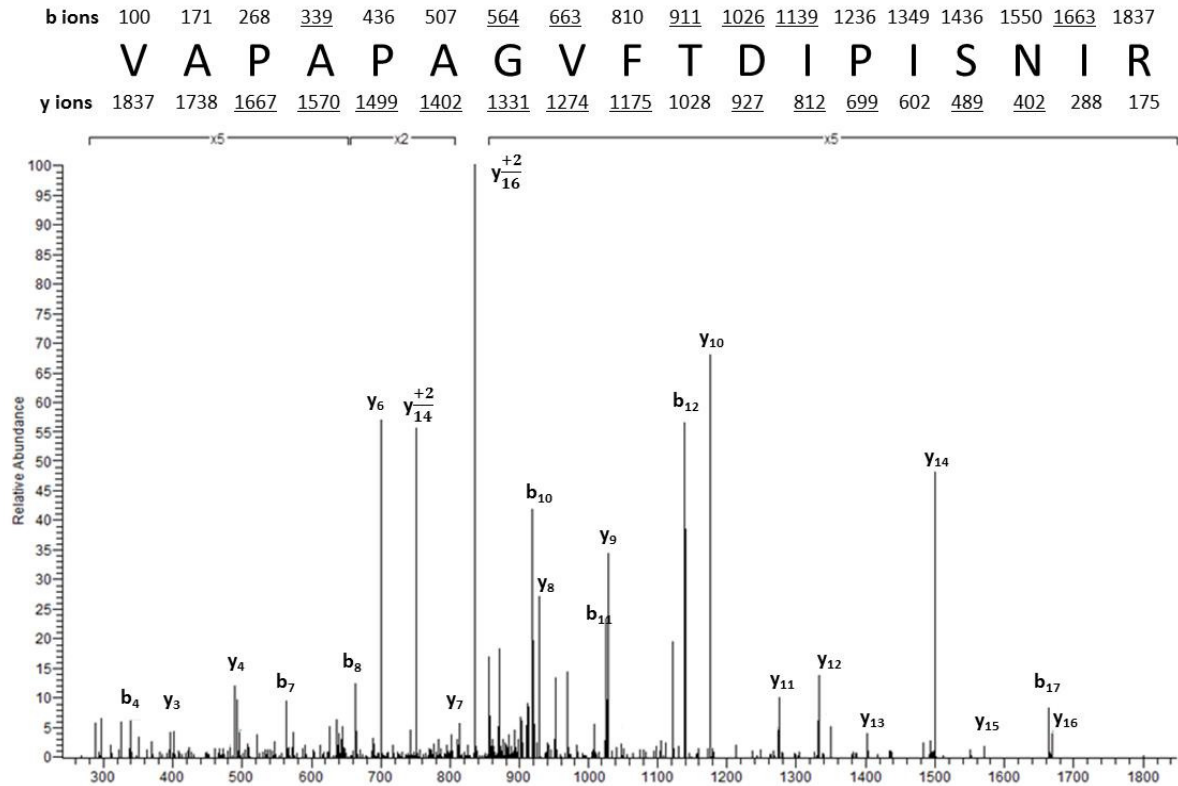


Figure 2.21. CID mass spectrum recorded on the $(M+2H)^{+2}$ ion at m/z 919. The sequence of the peptide is shown with the predicted y and b fragments. Ions observed in the spectrum are underlined.

A lot of the previous studies with C-peptide have identified an effect on the Na^+K^+ -ATPase activity of a cell. The Na^+K^+ -ATPase is inactive in its phosphorylated state and only becomes activated when the phosphate group is removed by a phosphatase enzyme (see Figure 2.4). The phosphatase enzyme contains a cysteine residue in its active sites that is susceptible to oxidation and can serve as a redox sensor for a cell. In an oxidative environment, this cysteine can become oxidized, rendering the phosphatase inactive and preventing the activation of the Na^+K^+ -ATPase. The dihydrolipoyllysine-residue acetyltransferase (E2) has lipoyic acid groups attached to select lysine residues through an amide bond (Figure 2.22). In future experiments, we plan on isolating more of this protein to confirm the presence of lipoyl groups attached to the

protein and to identify which lysine residues within the protein are modified with a lipoyl group. Lipoic acid can be synthesized from octanoic acid. The octanoic acid is already bound to enzyme complexes prior to the insertion of the sulfur atoms, so no biologically synthesized lipoic acid would be found in a “free” state in cells. Lipoic acid is a known antioxidant that protects cells against damage. A few studies have suggested that alpha-lipoic acid supplements may enhance the body's ability to use its own insulin to lower blood sugar in people with Type-2 diabetes and may help to reduce the symptoms of peripheral neuropathy. Hyperglycemia-induced oxidative stress induces programmed cell death of nerves, that contributes to the pathology of diabetic neuropathy.²⁵ Lipoic acid was also shown to increase the amount of intracellular glutathione (GSH)²⁶ and has been shown to be a powerful free radical scavenger. As diabetes has been associated with increased production and/or decreased clearance of ROS, oxidative stress has been suggested to contribute to oxidative damage leading to the complications associated with diabetes. Therefore, the lipoyl groups attached to the E2 protein may play an important role in reducing the level of ROS within a cell. Our experimental results have led us to hypothesize that the C-terminal isoform of the E2 enzyme may have an antioxidant role in protecting tissues with higher exposure to oxidizing agents like the kidneys and that the C-peptide may activate these antioxidant properties of the E2 protein by perhaps binding and causing a conformational change that further exposes the lipoyl groups attached to the protein. Further research will need to be conducted to prove this hypothesis.

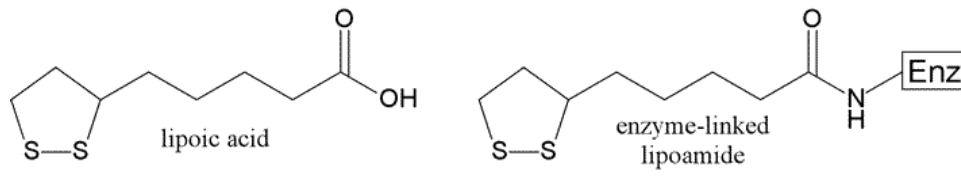


Figure 2.22. Structure of lipoic acid and its attachment to a lysine residue through an amide bond.

References:

1. Steiner, D.F., Cunningham, D., Spigelman, L., and Aten B. (1967). *Science*. 157 (3789), 697–700.
2. Marques, R.G., Fontaine, M.J., and Rogers J. (2004). *Pancreas*. 29(3),231-8.
3. Kim, C.S., Nam, J.H., Nam, J.S., et al. (2006) *Metabolism*. 55(8),1107-12.
4. Shiraj, E., Reddy, S., Scherbaum, W.A., Abdulkadir, J., Hammel, J.P., and Faiman C. (2002). *Diabetes Care*. 25,453-57.
5. Wahren, J., et al. (2000) *Am J Physiol Endocrinol Metab*. 278(5),E759-68
6. Ido Y, et al. (1997) *Science*. 277(5325),563-6
7. Rigler. R, et al. (1999) *Proc Natl Acad Sci U S A*. 96(23),13318-23.
8. Lebherz, Corinna, and Marx, N. (2013) *Curr Atheroscler Rep* 15,339 1-9.
9. Panero, F., Novelli, G., and Zucco, C. (2009). *Diabetes Care*. 32,301
10. Johansson, B.L., Wahren, .J, and Pernow, J.(2003) *Am J Physiol Endocrinol Metab*. 285,E864-70
11. Ekberg, K., Brismar, T., and Johansson, B.L. (2007) *Diabetes Care*. 30,71–6
12. Johansson, B.L., Borg, K., and Fernqvist-Forbes, E. (2000) *Diabet Med*. 17,181–9
13. Patel, N., Taveira, T.H., and Choudhary, G.(2012) *J Am Heart Assoc*. 1,e003152.
14. Sari, R., and Balci, M.K.(2005). *J Natl Med Assoc*.5,97,1113–8.
15. Irwin, M.L., Duggan, C., and Wang, C.Y.(2011) *J Clin Oncol*.29,47–53.
16. Bhatt, M.P., Lim, Y.C., and Hwang, J.(2013) *Diabetes*.62,243–53
17. Shafqat, J., Melles, E., Sigmundsson, K. et al. (2006) *Cellular and Molecular Life Sciences* .63,1805-11.

18. Lindahl, E., Nyman, U. , Melles, E., Sigmundesson, K., and Stahlberg., M. (2007) *Cellular and Molecular Life Sciences* 64,479-86.
19. Kennedy, R.T., and Jorgensen, J.W.(1989) *Analyt. Chem.* 61, 1128-1135.
20. Morita, K., Saruwatari, J., Miyagawa, H., et al. (2013) *Cardiovasc. Diabetol.* 12, 132.
21. Chen, C.H., Ferreira, J.C., Gross, E.R., and Mochly-Rosen, D. (2014) *Physiol. Rev.* 94, 1-34.
22. Gao, Q., Wang, H.J.; Wang, X.M., et. al (2013) *Food and Chemical Toxicology* 56, 419-424.
23. Ha, H., Hwang, I., Park, J.H., and Lee, H.B.(2008) *Diabet Res Clin Pract* 82, 42-45.
24. Lara, P.C., Pruschy, M., Zimmerman, M., and Hernandez, L.A. (2011) *Radiat Oncol.* 6, 148.
25. Zimmer, G. In: Fuchs, J., Packer, L., Zimmer, G., editors. (1997)*Lipoic acid in health and disease.* 67–86.
26. Busse, E., Zimmer, G., Schopohl, B., Kornhuber, B. and *Arzneimittelforschung.* (1992)42,829–831

Appendix A:

Results from Earlier Trials for Heart Tissue Lysates:

In an early trial, an alternative form of C-peptide that still contained the RR and KR amino acids on the termini of the peptide was used to generate the C-peptide beads. This peptide was chosen in the hope that the extra primary amine in the additional lysine residue would bind to the NHS beads, leading to binding at both ends of the peptide as opposed to only through the N-terminus. Mouse heart, liver, and kidney tissue was lysed with NP-40 lysis buffer, pre-cleared with Tris beads, and incubated with C-peptide beads overnight at 4° C. The isolated proteins were then separated by SDS-PAGE electrophoresis (Figure A.1). For this trial, the kidney and liver lanes of the gel were too overloaded to identify any protein binding partners, but the mouse heart lane had several proteins that could be identified via Peptide Mass Fingerprint.

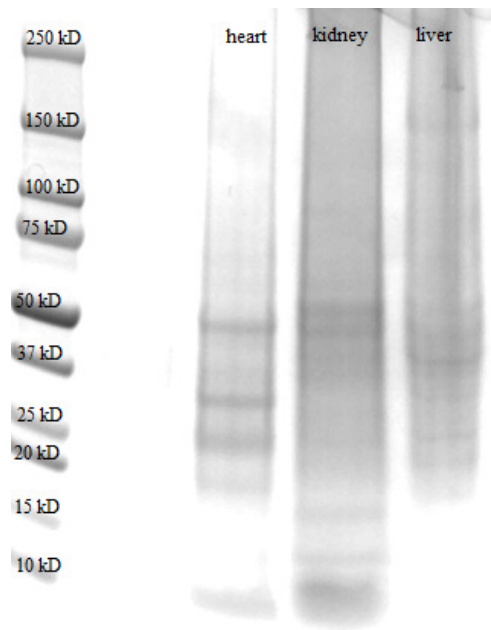


Figure A.1. SDS-PAGE gel of proteins isolated with C-peptide beads from mouse heart lysate, mouse kidney lysate, and mouse liver lysate. Protein bands from the heart lane were excised from the gel for further analysis.

The protein band at about 55 kDa was excised from gel, digested with trypsin, and analyzed by MALDI-TOF mass spectrometry (Figure A.2). The protein was identified as ATP synthase subunit alpha. The purpose of this protein is to produce ATP from ADP in complex V in the electron transport chain using a proton gradient across the membrane that is generated by electron transport complexes of the respiratory chain. Unfortunately, this protein was found in subsequent trials using the NHS magnetic beads in the pre-clear lanes, indicating it has an affinity for the NHS beads themselves and not C-peptide.

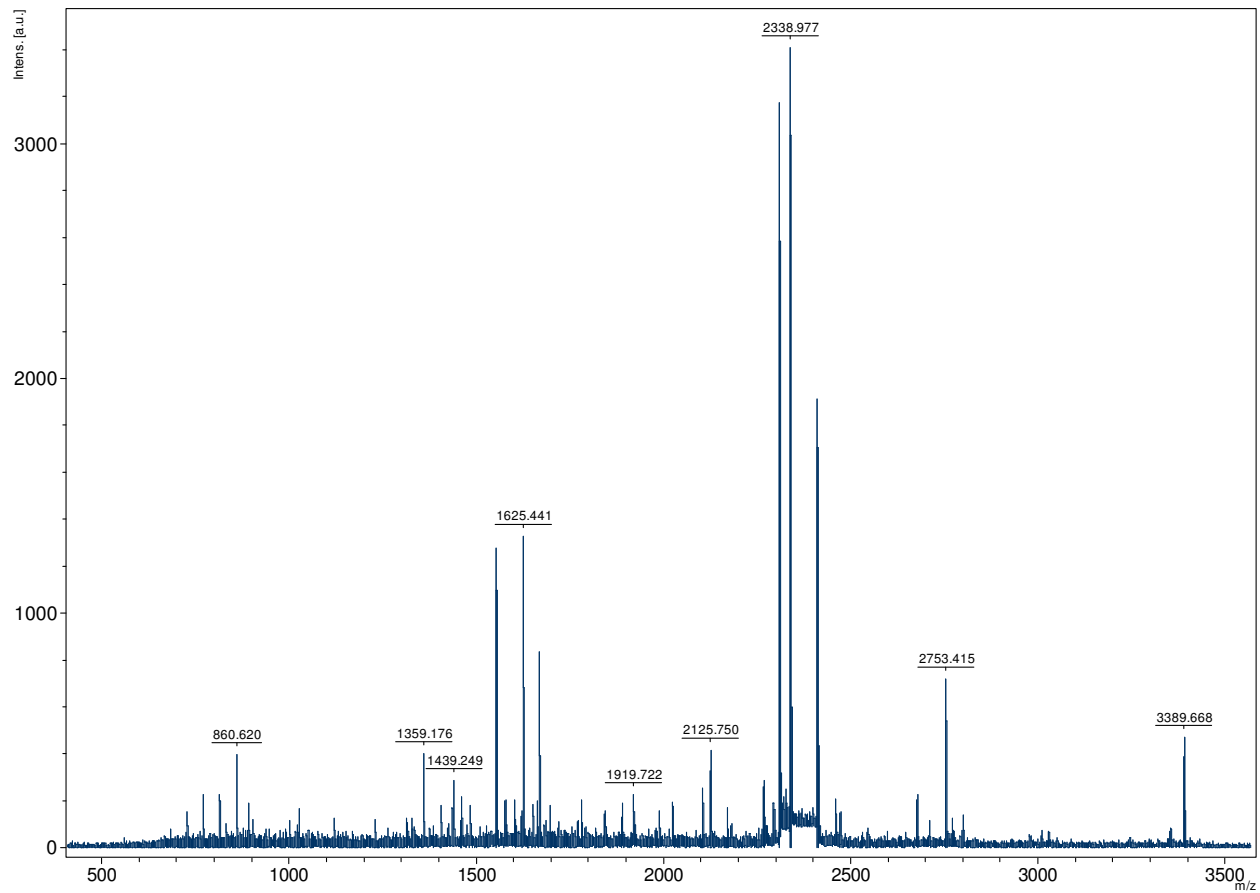


Figure A.2. MALDI-TOF peptide fingerprint mass spectrum for the protein excised from the band at 55 kDa in the heart lysate lane in the SDS-PAGE gel in Figure A.1.

The protein band at about 30 kDa was also excised from gel, digested with trypsin, and analyzed by MALDI-TOF mass spectrometry (Figure A.3). The protein was identified as glyceraldehyde-3-phosphate dehydrogenase (GAPDH). This enzyme catalyzes the sixth step in glycolysis, serving to breakdown glucose for energy, specifically the reaction of glyceraldehyde 3-phosphate to D-glycerate 1,3-bisphosphate (Figure A.4). C-peptide may bind to GAPDH to help activate the break down of glucose. This would make sense since insulin and C-peptide are released from the pancreas when blood glucose levels are high. Throughout our C-peptide trials, we isolated this protein once again from liver tissue, and we never identified this protein from

any pre-clear samples. This protein remains a good candidate as an effector protein of the C-peptide; however, additional trials need to be conducted to confirm this result.

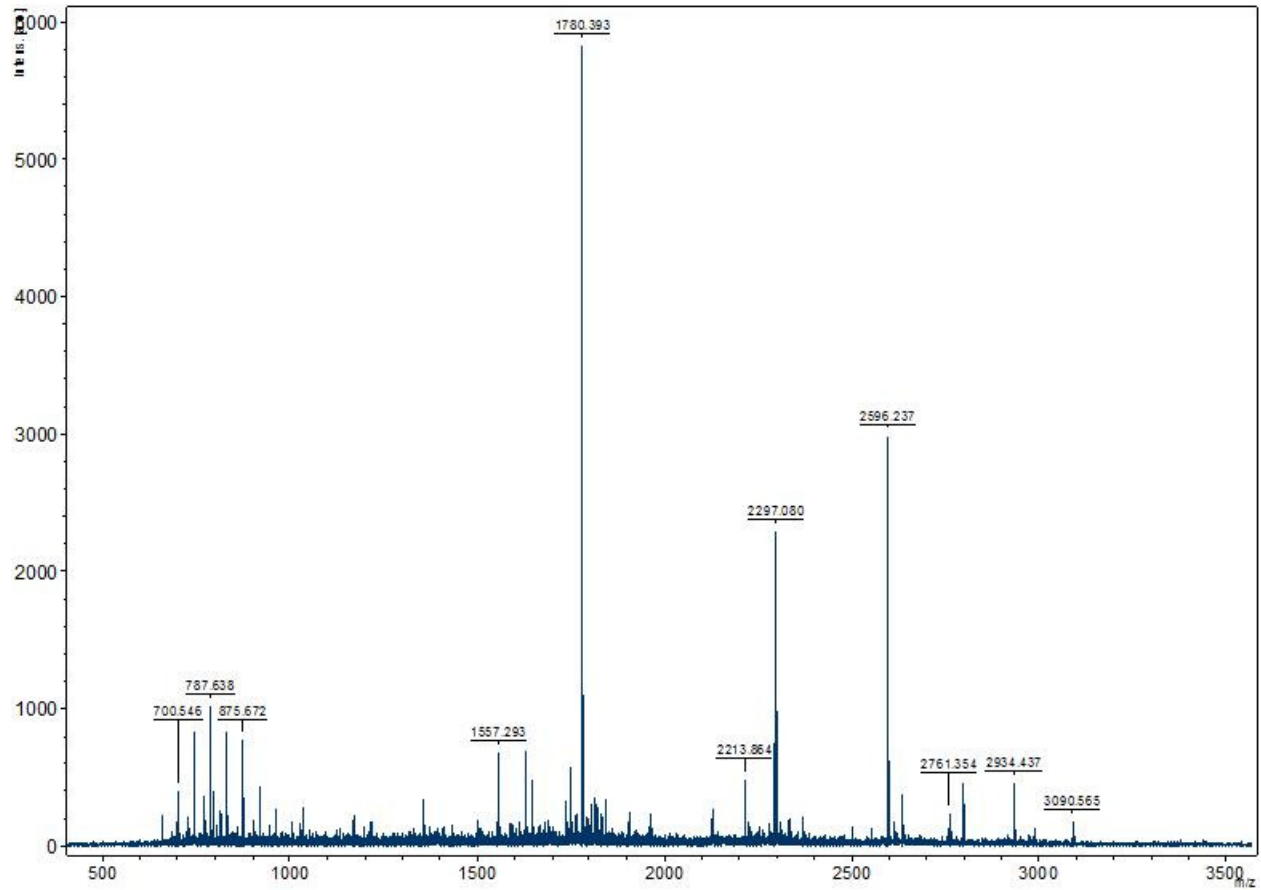


Figure A.3. MALDI-TOF peptide fingerprint mass spectrum for the protein excised from the band at 30 kDa in the heart lysate lane in the SDS-PAGE gel in Figure A.1.

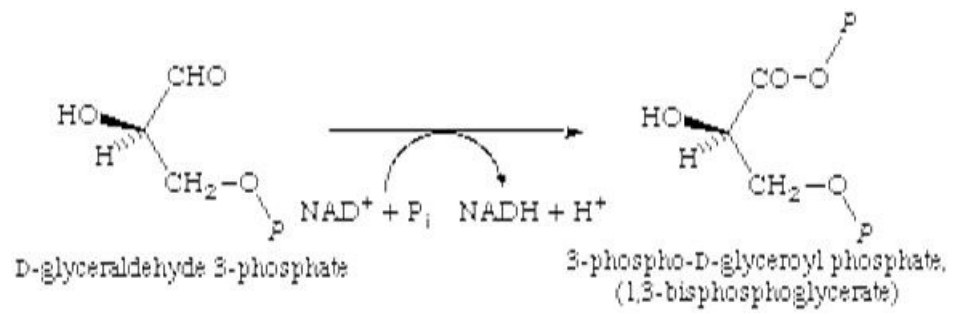


Figure A.4. The reaction catalyzed by GAPDH as part of the glycolysis cycle.